COO-2007-78

DEMONSTRATION OF THE FIRST VISIBLE WAVELENGTH DIRECT NUCLEAR PUMPED LASER

by

MARVIN ALFRED AKERMAN

NUCLEAR ENGINEERING PROGRAM

UNIVERSITY of ILLINOIS at URBANA-CHAMPAIGN

URBANA, 1976

DISCLAIMER

DEMONSTRATION OF THE FIRST VISIBLE WAVELENGTH DIRECT NUCLEAR PUMPED LASER

BY

MARVIN ALFRED AKERMAN

B.S., University of Virginia, 1968
M.S., University of Illinois, 1974

THESIS

Submitted in partial fulfillment of the requirements
for the degree of Doctor of Philosophy in Nuclear Engineering
in the Graduate College of the
University of Illinois at Urbana-Champaign, 1976

Urbana, Illinois

DEMONSTRATION OF THE FIRST VISIBLE WAVELENGTH DIRECT NUCLEAR PUMPED LASER

Marvin Alfred Akerman, Ph.D.
Nuclear Engineering Program
University of Illinois at Urbana-Champaign, 1976

This study describes the first direct nuclear pumped laser to operate on a visible wavelength, whereas previous nuclear lasers have operated in the infrared. The Sandia Pulsed Reactor II was used as a high flux source of neutrons that pumped a helium-mercury gas laser via the high energy products of the $^{10}B(n,\alpha)^{7}Li$ nuclear reaction. No other source of energy was utilized. Lasing was observed at 6150 Å, corresponding to the $7^2P_{3/2}-7^2S_{1/2}$ mercury ion transition.

The thermal neutron flux threshold for lasing was ~$1X10^{16}$ n/cm^2-sec, and the laser output was continuous over the 400 μsec operating time of the nuclear reactor. The laser signal appeared to increase linearly with the thermal neutron flux, up to $5.8X10^{16}$ n/cm^2-sec, the highest flux used.

With the limited number of reactor pulses available, experiments concentrated on mercury partial pressures in the range 2 to 10 mTorr at a total pressure of 600 Torr. The laser output increased as the mercury partial pressure was decreased, with an apparent saturation beginning at ~2.5 mTorr. A single data point at 300 Torr total pressure and 2.5 mTorr showed a decrease in the laser output. To investigate possible lasing at higher mercury pressures as suggested by earlier workers, the total pressure was adjusted to 350 Torr with 2.8 Torr mercury partial pressure, but no lasing was observed at 6150 Å.

The peak power output for the present device was ~1mW. This corresponds to an efficiency of only 10^{-6}%, but the laser was not

designed for maximum efficiency or power. Consequently, it is thought to be possible to design systems that come closer to the theoretical quantum efficiency of 8% if this were a goal.

In addition to the laser experiments, gain measurements are described that use a chopped resonant cavity spectroscopy technique at a neutron flux too low to produce lasing. The gain measurements, which were made using the University of Illinois TRIGA reactor as a pulsed source of neutrons, successfully predicted the operating regime of the DNPL achieved while using the Sandia SPR II reactor. A maximum gain was found at Hg partial pressures ~3 mTorr and 600 Torr total pressure, in general agreement with the limited laser data points. The decrease in gain, or laser output, with increasing Hg partial pressure is not fully understood. However at the higher total pressures, the decreasing gain with mercury pressure is thought to occur via a complicated mechanism involving competition between charge-exchange, He_2^+ formation, and Penning reactions.

The discovery of the 6150 Å helium-mercury direct nuclear pumped laser demonstrates the feasibility of nuclear pumping at visible wavelengths. An understanding of the mechanisms involved in exciting this laser may lead to higher efficiency visible and ultraviolet DNPLs which may ultimately be applied in the areas of laser fusion, isotope separation, communications and energy removal from gas core nuclear reactors.

ACKNOWLEDGMENT

Thanks are due Professor G. H. Miley, who suggested the present research and supported it with constant funding and ideas. Many conversations with W. E. Wells, who first proposed that He_2^+ formation could be important in the He-Hg DNPL, are appreciated. J. T. Verdeyen was a source of encouragement and aid from the beginning. D. A. McArthur invited me to use Sandia Laboratories' fast burst reactor and scheduled the two-week period for my experiment in July 1976. His efforts are sincerely appreciated.

K. Kuehl, E. Boose and A. Wilson of the U. of I. Electrical Engineering Department Special Processes Laboratory are thanked for constructing the Pyrex tube and electrode assembly of the lasers.

The assistance of a number of graduate students, including J. Anderson, G. Cooper, M. Konya and M. Prelas is appreciated.

G. King and O. Croft helped a great deal setting up the lasers and associated equipment at the Sandia Labs SPR II facility. The cooperation of the SPR II staff members is also acknowledged.

G. Beck, P. Hesselmann, C. Pohlod and D. Sigler are thanked for pulsing the U. of I. TRIGA reactor, where much of this work was accomplished.

The research was funded by a grant from the Physical Research Division of ERDA. This support is gratefully acknowledged.

The Nuclear Engineering Program staff, including the personnel of the drafting department, electronics shops and machine shop and the clerks and secretaries are thanked sincerely. In particular, J. Borchers, C. Johnson, P. Roosevelt and L. Stalker were of immense help.

During four years of false starts, glass breaks and vacuum leaks, my wife, Margo, never faltered. Her positive attitude and help from beginning to end made the He-Hg DNPL discovery possible. Our daughter Doriann arrived for the final year of this research and was a lovable diversion.

TABLE OF CONTENTS

I. INTRODUCTION

The advent of the Direct Nuclear Pumped Laser (DNPL) is recent. Only in 1974 was the first such laser developed. It used carbon monoxide and was pumped by neutrons from the Sandia Fast Burst Reactor.[1] Later, other gas mixtures, including helium-xenon, neon-nitrogen and helium-argon, were utilized to produce DNPLs.[2-4]

The expression, "Direct Nuclear Pumped," is used to identify and set apart a class of lasers whose sole source of power is the products of nuclear reactions. Reviews of previous DNPL research may be found in Refs. 5-9.

A. Goals of This Study

The helium-mercury laser experiments described here were begun in 1973. At that time there were no nuclear pumped lasers, only theoretical models that predicted their feasibility.

The helium-mercury mixture was chosen for two reasons. The first was that the 6150-Å mercury-ion laser transition had all of the properties thought at that time important in making a DNPL. These properties are discussed in detail in Chapter II. The second was that a paper published by Soviet researchers in 1969 hinted that they might have achieved lasing on the 6150-Å transition, though they gave no proof.[10] Subsequent attempts to measure gain at the Soviet gas partial pressures with both ^{3}He and ^{10}B excitation methods met with no success.[11] A careful duplication of their reported lasing conditions also met with no success. It was with far lower mercury pressures that the helium-mercury DNPL actually was discovered.[12] This thesis describes the operation of the 6150-Å laser, the first visible DNPL, discovered in July 1976 by this researcher. It also includes gain measurements that predicted the optimum

lasing conditions, and minimum pumping power estimates that support the conclusions of both the gain and the laser experiments.

B. Review of Previous He-Hg Electrical Studies

The 6150-Å mercury-ion laser was discovered in 1963 by W. E. Bell.[13] Since then, other researchers have studied gain,[14,15] the effect of helium,[16] hollow cathodes,[14,17,18] and other mercury lasers.[18-22]

Several recent measurements of the charge exchange cross section have been reported in the literature.[16,23-25] Two others show charge exchange is the populating mechanism in the 6150-Å laser, but do not measure the cross section.[26,27]

These studies are in basic agreement with a 1965 report that charge-exchange is the dominant populating mechanism of the upper laser level in the helium-mercury electrically pumped 6150-Å laser.[28] However, a Japanese researcher has shown that Penning ionization is responsible for populating the upper laser level, not charge exchange.[29] Differences in experimental conditions could be responsible for this apparent contradiction.

Two other papers resulting from the present research deal with the nuclear radiation enhancement of an electrically operating helium-mercury laser.[30,31] This material is summarized in Appendix A.

C. Power Deposition

The excitation in the DNPL discussed here is accomplished by the products of a nuclear reaction. Thermal neutrons react with ^{10}B to form an unstable nucleus. This splits to form highly energetic alpha and ^{7}Li particles:

$$n + {}^{10}B \rightarrow {}^{4}He + {}^{7}Li + 2.35\ MeV. \qquad (I\text{-}1)$$

These reaction products in turn produce high-energy electrons as a result of collisions with atoms in the gas. Approximately one tenth of the neutrons passing through the foil produce the energetic reaction products mentioned above. Approximately one fourth of these reaction products reach the gas and on the average cause 2,000 primary electrons per ion to be formed. Each primary electron creates up to 50 secondary electrons through ionizing collisions. So for every ion entering the gas, 100,000 secondary electrons may be formed. These secondary electrons then create a majority of the excited states in the gas at the pressures used in this research. At low pressure direct excitation is important.[32,33] A graph showing the relative energy deposited in helium by several different nuclear excitation schemes is shown in Fig. 1. The computations used to arrive at these curves are outlined in Appendix B. From Fig. 1 it can be seen that the ^{10}B foil provides more power to the gas at pressures below an atmosphere. A uranium coating could provide more power deposition than the ^{10}B coating in the same pressure range. The choice of the ^{10}B coating for the present experiment was made for convenience.

That nuclear excitation holds an advantage over the conventional means of electrical excitation at high pressure can be seen in Fig. 2. Here, the spectrum of a helium-mercury mixture similar to that used to achieve the DNPL is shown in the first column. The second column shows a spectrum for the same gas mixture, but with electrical excitation. The mercury-ion lines at 6150 Å and 2848 Å are apparent in the first column, and the last column, where excitation was electrical at low

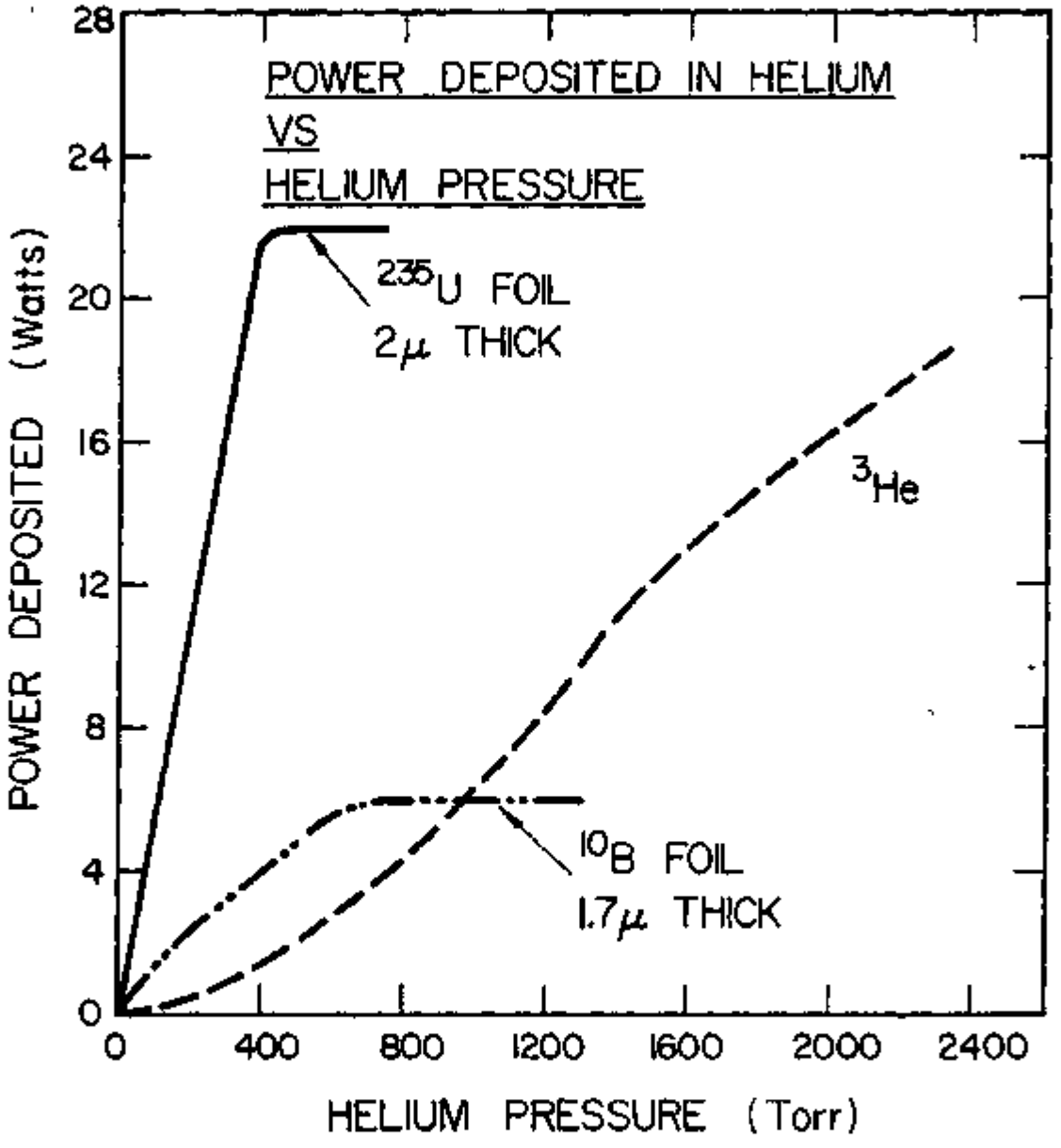

Fig. 1. Relative energy deposited in helium figured by three nuclear excitation schemes.

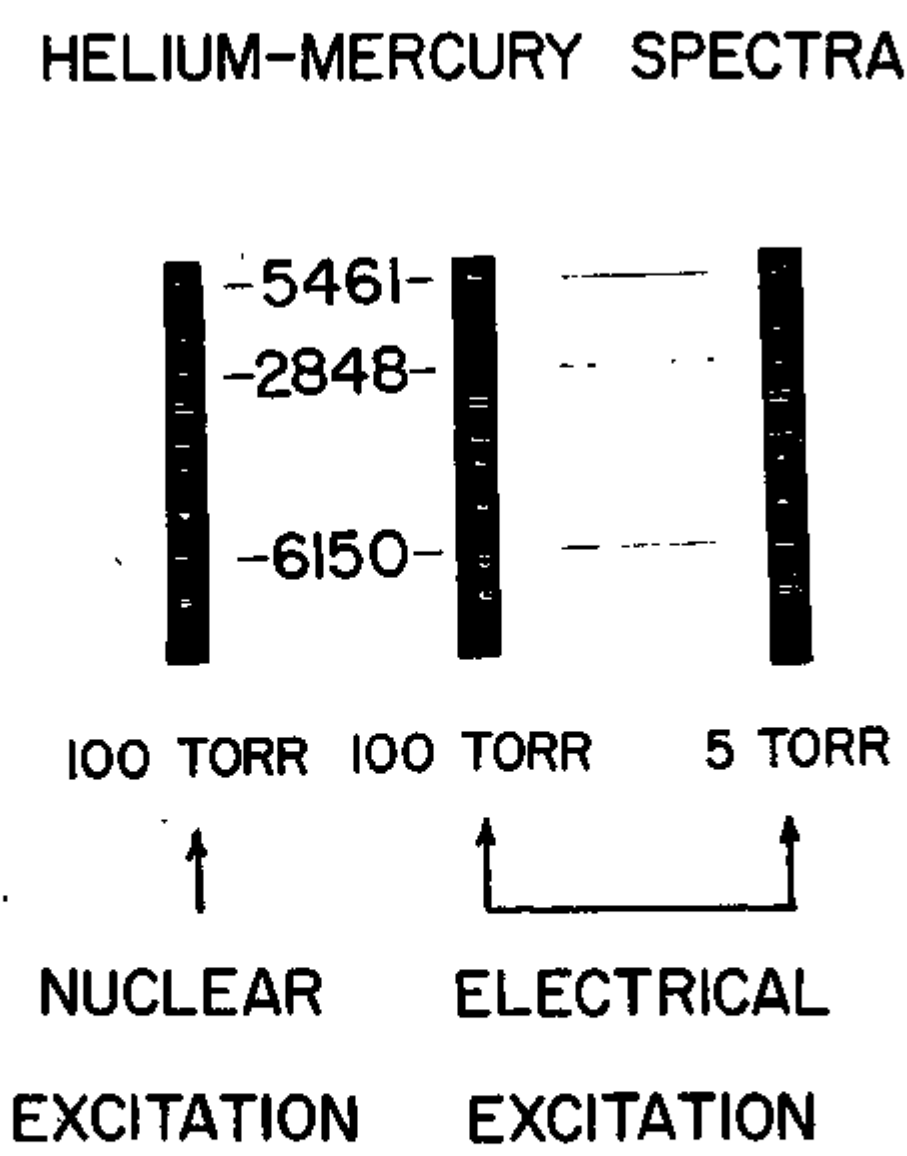

Fig. 2. Comparison of three helium-mercury spectra shows that high pressure nuclear excitation produces more 6150-Å light than high pressure electrical excitation relative to other lines.

helium pressure. The middle column, electrical excitation at relatively high pressure, shows that electrical excitation cannot compete with nuclear excitation in the relative efficiency with which ion states are produced at high pressure.

The two lines in the middle spectrum appearing just below the 6150-Å marker are the 3082-Å and 3093-Å lines from excited aluminum atoms. These are knocked off the electrodes in the high pressure discharge.

D. Review of Previous DNPL Work

Table 1 lists the previous DNPLs discovered using research reactors. Carbon monoxide was used to develop the first DNPL. Research is continuing to optimize its output, and to show the feasibility of scaling to larger devices and higher power output.[34] The second DNPL used a helium-xenon mixture and produced a much lower power output.[2] Two lines were identified in a third discovery at the University of Illinois using a neon-nitrogen mixture.[3] Helium-3, a volume source of nuclear excitation, was used to produce the fourth DNPL in a helium-argon mixture.[4]

Each of these lasers operates in the infrared, though the wavelength of the neon-nitrogen laser is short enough to be detected using standard photomultipliers.

The helium-mercury DNPL reported in this thesis is the first to operate at a visible wavelength.

Other experiments have utilized atomic bomb blasts to pump gas lasers.[35,36] These were excited by prompt gamma rays and ran from the initiation of the blast until the destruction of the laser.

NUCLEAR PUMPED LASERS	PUMPING REACTION	WAVELENGTH	THERMAL FLUX THRESHOLD (n/cm^2-sec)	LENGTH OF LASER OUTPUT	PEAK LASER POWER
He-Hg UNIV. OF ILLINOIS SANDIA LABS	$^{10}B(n,\alpha)^{7}Li$	6150 Å	$\sim 1 \times 10^{16}$	400μsec	~1 mW
CO SANDIA LABS	$^{235}U(n,F)FF$	5.1-5.6μ	$\sim 5 \times 10^{16}$	50μsec	2-6 W
He-Xe LOS ALAMOS UNIV. OF FLORIDA	$^{235}U(n,F)FF$	3.5μ	3×10^{15}	150μsec	>.01 W
Ne-N_2 UNIV. OF ILLINOIS	$^{235}U(n,F)FF$ and $^{10}B(n,\alpha)^{7}Li$	8629Å and 9393Å	1×10^{15}	6 m sec	1.5 mW
^{3}He-Ar NASA LANGLEY	$^{3}He(n,p)T$	1.79μ	1.4×10^{16}	365μsec	50 mW

Table 1. A summary of DNPL's that have been discovered with research reactors as of July, 1976.

Gain measurements have also been made in the research nuclear reactor environment. These are, in many respects, more difficult than DNPL experiments because of the alignment and low light-level detection necessary. Thermal focusing can also be a problem.[37] The three reported gain measurements are shown in Table 2. Of the three, the first and the last have led to a DNPL, while the second is being optimized in the hopes of achieving a DNPL.[38-39,11]

DNPL research is growing rapidly in the United States. Since 1974, the number of laboratories working on some phase of the DNPL has almost tripled. The usefulness of such a device as a compact, high energy, coherent light source is gaining recognition. DNPLs could have many applications. They could be valuable for high efficiency energy conversion, laser isotope separation, laser fusion or energy removal from gas core nuclear reactors.

NUCLEAR-INDUCED GAIN MAY 1976	PUMPING REACTION	WAVELENGTH	REMARKS
CO SANDIA LABS	$^{235}U(n,F)FF$	5.1-5.6μ	LASING ACHIEVED (SEE LASER TABLE)
$^{3}He-Ne-O_2$ UNIV. OF ILLINOIS	$^{3}He(n,p)T$	8446 Å	
He-Hg UNIV. OF ILLINOIS	$^{10}B(n,\alpha)^{7}Li$	6150 Å	LASING ACHIEVED (SEE LASER TABLE)

Table 2. A summary of reported DNP gain measurements.

II. DESCRIPTION OF ATOMIC PROCESSES

Two resonant processes for producing the upper laser level will be described, along with several other atomic processes. A minimum threshold population inversion will be calculated. An estimate of the population inversion with reactor conditions is compared to this minimum.

A. Laser Pumping Mechanisms

The $7^2P_{3/2}$ state and the $7^2S_{1/2}$ state of singly ionized mercury are shown in Fig. 3. These are the upper and lower laser levels for the 6150-Å transition. In Fig. 3 it can be seen that there is an energy coincidence between the helium ion and the $7^2P_{3/2}$ state of singly ionized mercury. This coincidence leads to a large cross section for charge transfer:[23]

$$He^+ + Hg \rightarrow Hg^+ (7^2P_{3/2}) + He + K.E. \qquad (II\text{-}1)$$

In addition, Penning ionization can produce the same upper state:[29]

$$He^*(2^3S) + Hg^*(6^3PO) \rightarrow Hg^+(7^2P_{3/2}) + Hg + e^-(K.E.) \qquad (II\text{-}2)$$

The lifetimes of the upper and lower mercury states, 1.1×10^{-8} and 2.7×10^{-9} seconds respectively, are favorable for lasing.[40] The subsequent transitions to the mercury ground state ion are fast and, hence, facilitate the emptying of the $7^2S_{1/2}$ level.

B. Threshold Population Inversion

The threshold inversion density can be calculated as follows:

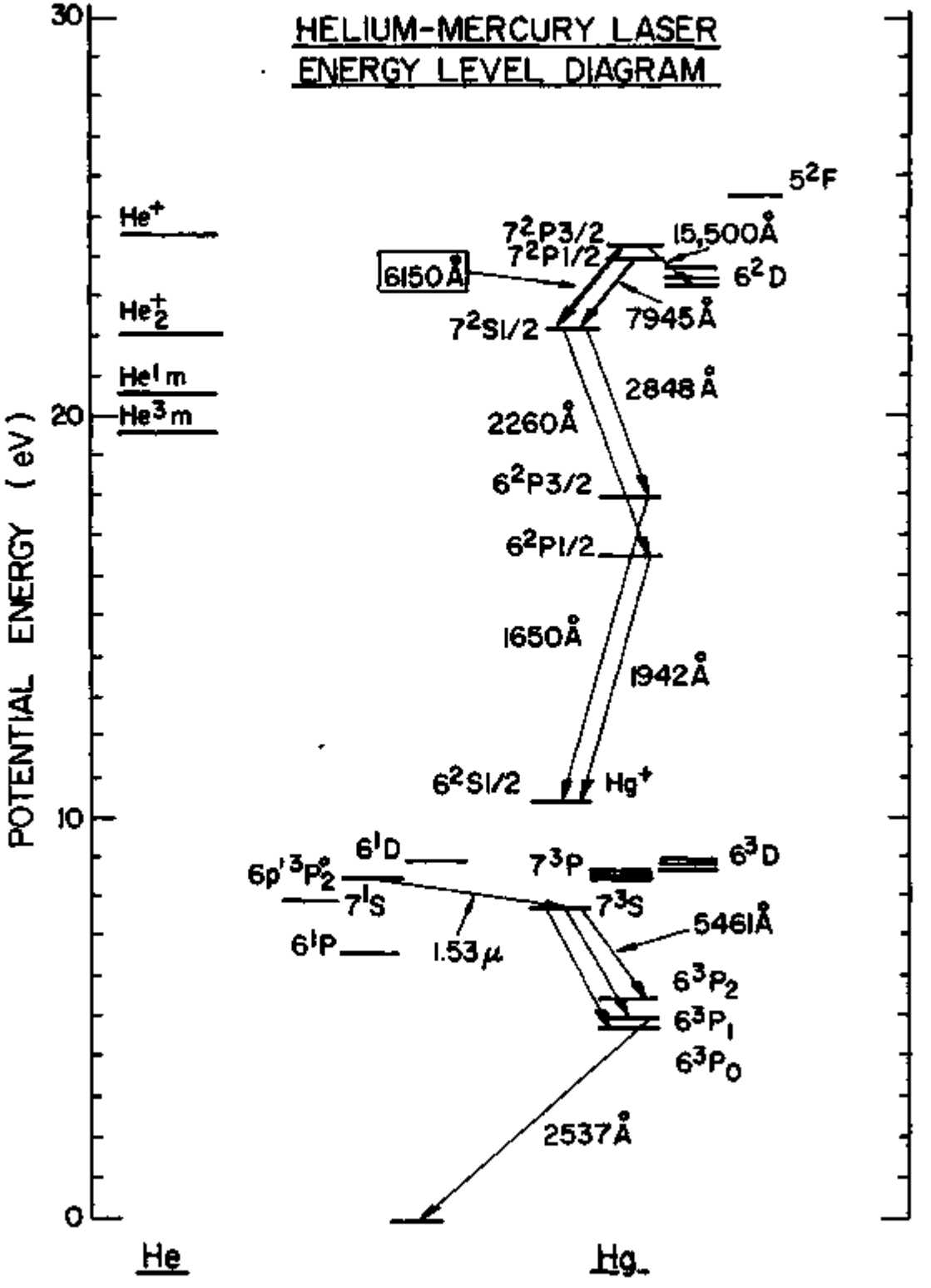

Fig. 3. A helium-mercury energy level diagram showing the 6150-Å transition.

$$n_{7P} - n_{7S}\frac{g_{7P}}{g_{7S}} = \frac{8\pi\tau_s}{c\lambda^2 g(\nu_0)\tau_p}$$

$$\sim \frac{(8)(\pi)(10^{-8}\text{sec})}{(3\text{x}10^{10}\text{cm/sec})(6.15\text{x}10^{-5}\text{cm})^2(2.3\text{x}10^{-10}\text{sec})(10^{-7}\text{sec})}$$

$$\sim 1\text{x}10^{8}\ \text{states/cm}^3. \qquad \text{(II-3)}$$

The photon power at threshold is related to the inversion density by:

$$P_{\text{minimum}} = (n_{7P} - n_{7S}\frac{g_{7P}}{g_{7S}})\frac{h\nu}{\tau_s}$$

$$\sim \frac{(1\text{x}10^{8}\ \text{states/cm}^3)(2\ \text{eV})(1.6\text{x}10^{-19}\ \text{Joule/eV})}{(10^{-8}\text{sec})}$$

$$\sim 3.7\text{x}10^{-3}\ \text{watts/cm}^3. \qquad \text{(II-4)}$$

where: n_{7P} = upper atomic energy level density

n_{7S} = lower atomic energy level density

τ_s = spontaneous lifetime of $7^2P_{3/2}$ level

τ_p = cavity lifetime = $L/RC \sim \frac{(100\ \text{cm})}{(0.04)(3\text{x}10^{10})} = 10^{-7}$ sec

L = cavity length

R = cavity loss/path

c = speed of light

λ = transition wavelength = 6149.5 Å.[41]

For a collision broadened line profile at 600 Torr:

$$g(\nu_0) \sim \frac{1}{\Delta\nu} = 2.4\text{x}10^{-10}\text{sec}$$

$$\Delta\nu \sim 4.2\text{x}10^{9}\text{sec}^{-1}.[41]$$

It takes much more power than this to actually reach threshold since typically a great deal of the power deposited in the gas will excite other states and heat the gas.

C. $7^2P_{3/2}$ State Density

Rate equations were solved using estimates of the helium ion and helium metastable densities that could be produced with the University of Illinois TRIGA nuclear reactor. A model was used in which the nuclear reaction product energy goes predominantly into helium, and then is transferred to the mercury producing the upper laser level along with other excited states. This model does not reflect the behavior shown in Fig. 14 unless Penning ionization as well as charge exchange are considered. With charge exchange as the sole mechanism, one would expect an increase in 6150°A output with an increase in mercury partial pressure. This is observed in the low pressure hollow-cathode electrically operated laser for this range of mercury partial pressures. Therefore the two upper state populating mechanisms shown in Fig. 4 were included. In addition, the formation of He_2^+ and the possibility of charge exchange populating the lower level were evaluated.

Too many unknown densities and rates make a rigorous calculation of state densities impossible at this time. Nonetheless, steady state upper laser level densities and opulation inversion densities on the order of $10^9/cm^3$ were estimated for a neutron flux of $2.5X10^{15} n/cm^2$-sec. This estimate is an order of magnitude higher than the minimum threshold population inversion calculated in Section B, and indicates the feasibility of nuclear lasing with the experimental conditions described in Chapter III.

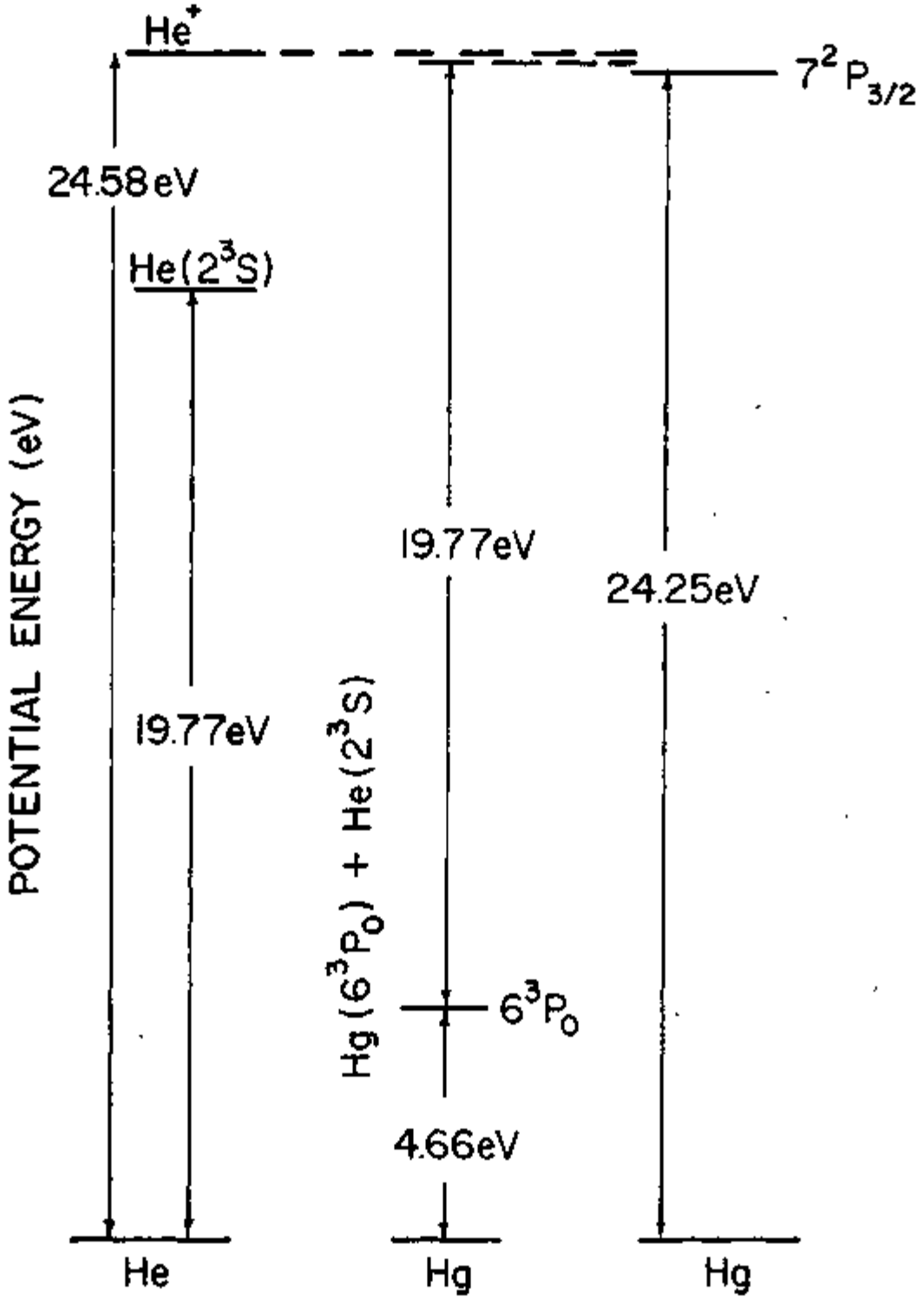

Fig. 4. The energy levels involved in two possible populating mechanisms $7^2P_{3/2}$ level are shown. These mechanisms are represented by equations II-1 and II-2.

III. EXPERIMENT DESIGN AND EQUIPMENT

A description of the laser used to produce the 6150-Å DNPL will be presented. Support equipment and the procedures used will be discussed.

A. The Laser Cell

The laser design, shown in Fig. 8,[17] was adapted for reactor use. Very nearly identical lasers were used for the gain experiments and the laser experiments. Both were constructed of 2.7-cm I.D. Pyrex, 86-cm long. High-temperature epoxy was used to seal thin Suprasil windows onto each end at Brewster's angle. A symmetrical hollow cathode and anode arrangement was employed to allow low-pressure electrical operation. The Pyrex outer tube was wrapped with three sets of heater tapes to control the mercury partial pressure, and three chromel-alumel thermocouples were placed between the heater tapes and the Pyrex to measure the temperature of the tube at several points.

The laser used for the gain experiments contained a 58-cm long aluminum hollow cathode that was coated to a 0.4 mg/cm^2 thickness on the inside with 90% enriched ^{10}B. This thickness is approximately equivalent to the range of an α-particle in boron. The anodes were each one centimeter lengths of the same material. The ^{10}B was factory applied in an oil suspension. To prepare it for laser use, the tubes were heated to 400°C and a vacuum was applied. Later, the Brewster windows had to be removed and cleaned after each reactor experiment. This implied that the tubes were still outgassing oil. About 70-100 milligrams of triple distilled mercury was placed inside the laser before it was sealed.

For the laser experiments at Sandia, a special hollow cathode was ordered. The cathode was a 60-cm length of 2.54-cm O.D. titanium tubing coated on the inside with a 0.4 mg/cm^2 layer of enriched ^{10}B. The ^{10}B

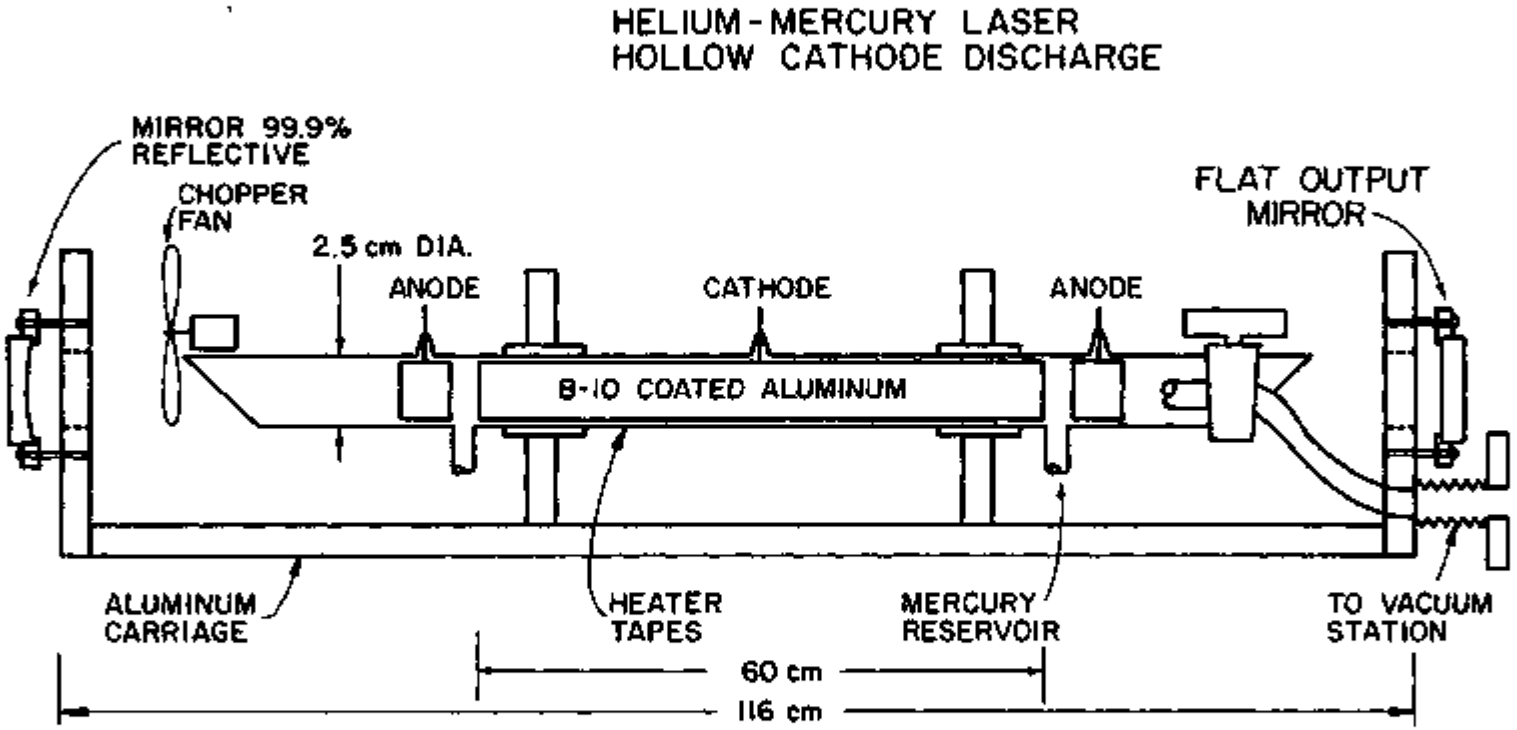

Fig. 5. Design of the laser cell used to produce the 6150-Å DNPL.

was applied in an oil and graphite suspension at the factory and baked for several hours at 700°C under a vacuum. The remaining mixture was 66.8% ^{10}B, 5.8% ^{11}B, and 27.4% graphite. Thus, for a given neutron flux, about 20% fewer ions/second will be deposited in the gas. A very small amount of oil was observed to come out of the tube during the initial clean up of the laser. However, it was nothing like the previous experience with oil suspension applied ^{10}B coatings. Two reservoirs contained a total of 79 milligrams of 67% isotopic abundance ^{202}Hg. The ^{202}Hg was used to increase the gain over that possible with naturally occurring mercury,[41] and to provide low impurity Hg vapor.

B. Illinois Experiments

1. Setup and Equipment

The basic experimental arrangement used for the gain measurements is shown in Fig. 9. The laser carriage was inserted three meters into the 14-cm diameter beamport of the University of Illinois TRIGA reactor and then attached to a large forepump and gas handling system.

The laser was operated in an electrically pulsed mode at low pressure to align the external optics and detector for a maximum amount of 6150-Å light at the detector.

A small, high-speed fan between the rear window and the back mirror of the laser was run at ~12,000 RPM during the reactor pulses, and this allowed the back mirror to be alternately blocked and unblocked.

2. Procedure

For approximately 15 minutes before nuclear reactor operation, the laser was open to the vacuum pump. During this time laser temperature changes were made to assure stability at pulse time. Five minutes before nuclear reactor operation, helium was metered into the system and the stopcock at the laser was closed. During nuclear reactor operation,

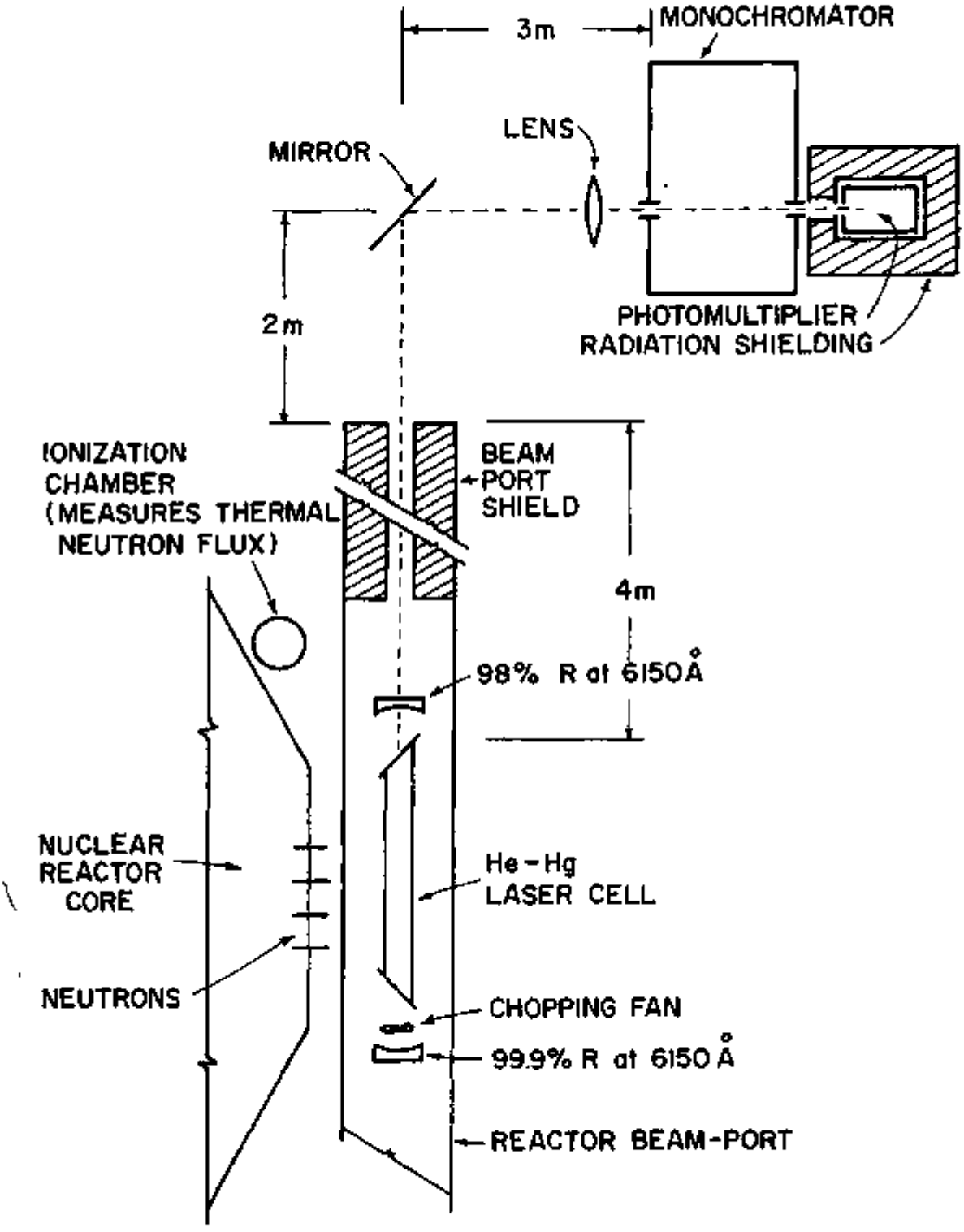

Fig. 6. Basic experimental arrangement used for gain measurements at the University of Illinois TRIGA reactor.

photomultiplier output was displayed on an oscilloscope and photographed. The output of a thermal neutron detector was also displayed and photographed. A timer between the reactor operations panel and the oscilloscopes was used to trigger the oscilloscopes approximately 20 milliseconds before reactor peak power. Approximately 20 minutes elapsed between pulses to allow the reactor to cool.

C. Sandia Experiments

1. Setup and Equipment

A laser of the same design and dimensions as the one used for the gain measurements was prepared and bolted into a rigid aluminum frame and mounted next to the Sandia Pulsed Reactor (SPR II). Figure 10 is a photograph of the laser in place on a Sandia experiment table. A one-inch thick cylinder of polyethylene, approximately 76 cm long, surrounded the centrally located ^{10}B-coated titanium cylinder. A stopcock controlled from outside the reactor shielding provided isolation of the heated laser from the vacuum station. The vacuum pumping and ultra-high-purity helium gas fill were controlled by remotely operated solenoids. A second laser of similar construction to the one described here is shown below the 6150-Å DNPL in Fig. 10. This laser was used for infrared DNPL experiments not discussed in this thesis.

With the laser and frame firmly locked into place, a 6328-Å helium-neon laser was aligned down the center of the nuclear laser tube. The arrangement is shown in Fig. 11. Mirrors were positioned to carry the alignment beam out of the reactor shielding through an 8-cm diameter opening, and then into a small room where a lens focused the light onto the photocathode of an RCA 31034 photomultiplier shielded on all sides by four inches of lead brick. With the optical path thus defined, the

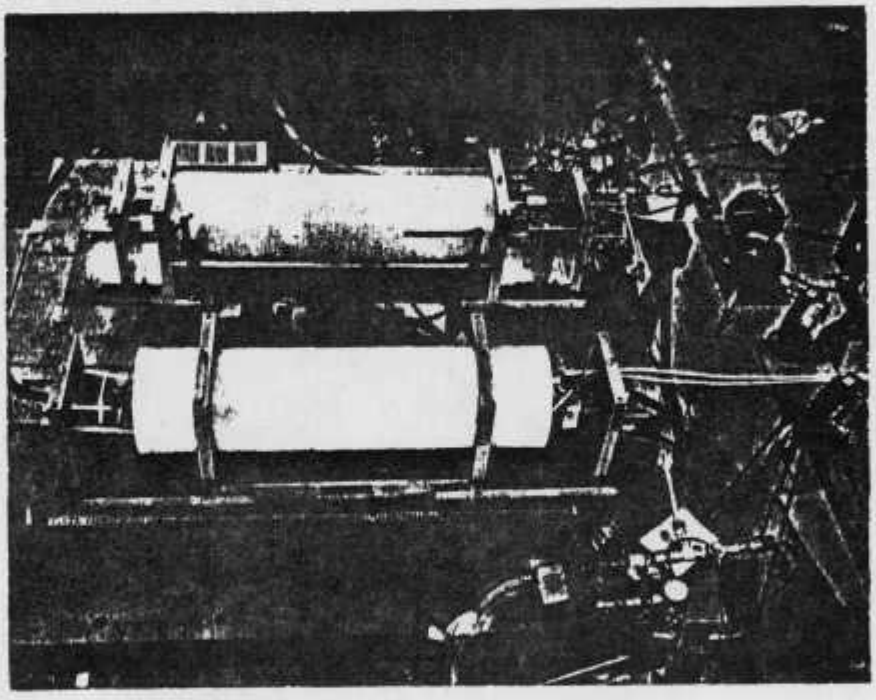

Fig. 7. Helium-mercury lasers in place on a Sandia Laboratory experiment table. The top laser is the 6150-Å DNPL.

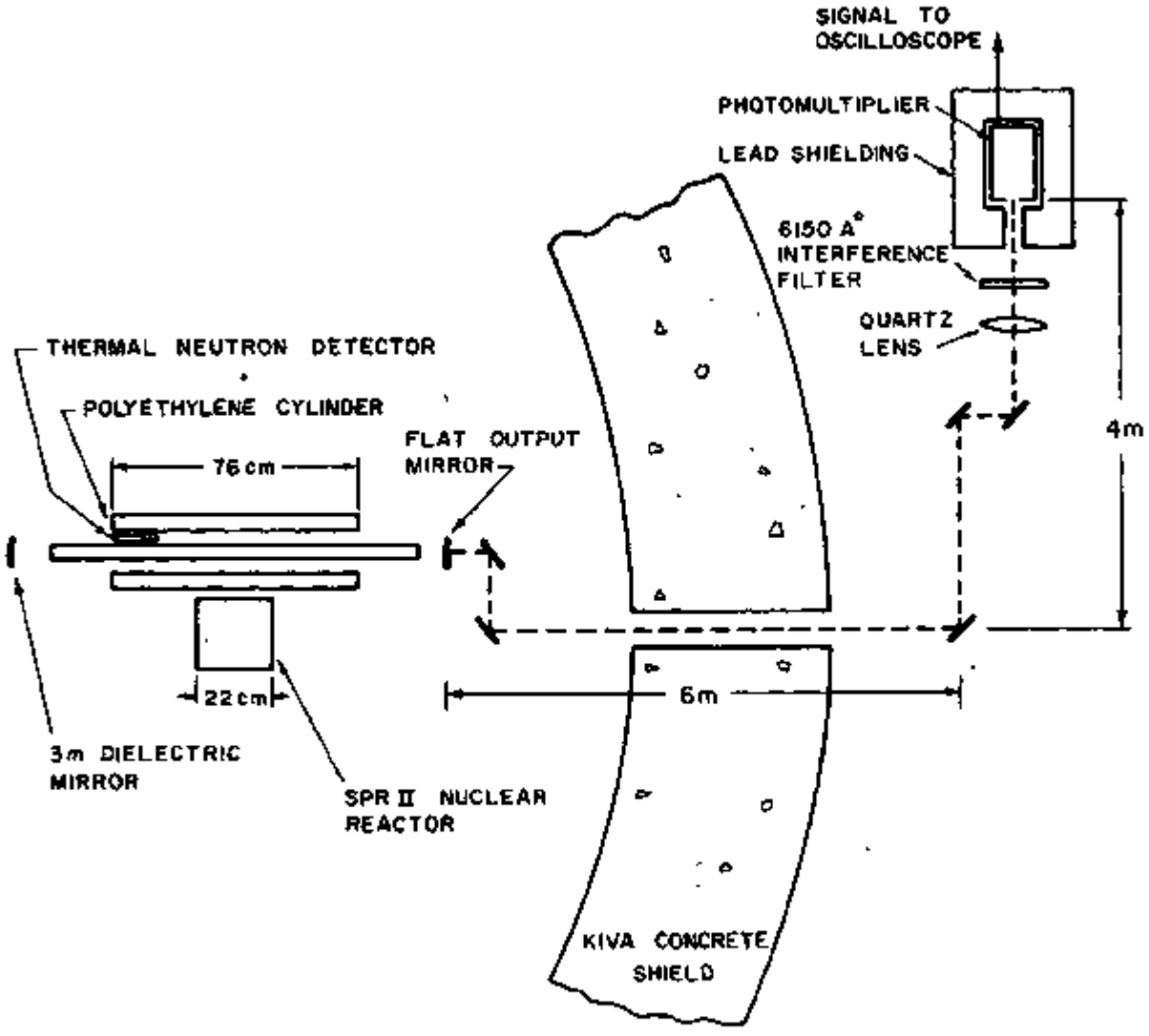

Fig. 8. Experimental arrangement used for DNPL experiments at Sandia Pulsed Reactor.

high-reflectivity dielectric laser mirrors were aligned on the same 6328-Å beam, and then finely aligned on the 6150-Å line of the mercury ion. A high Z preamplifier was used between the photomultiplier and the oscilloscope to improve time response despite the necessary 20 meters of connecting coaxial cable.

2. Procedure

For approximately 40 minutes before nuclear reactor operation, the laser was open to the vacuum pump. During this time laser temperature changes were made to assure stability at pulse time. Five minutes before nuclear reactor operation, helium was metered into the system and the stopcock at the laser was closed. During nuclear reactor operation photomultiplier output was displayed on an oscilloscope and photographed. The output of a high energy neutron detector and a thermal neutron detector were also displayed and photographed. A signal initiated by reactor power level was used to trigger the oscilloscopes approximately 300 microseconds before reactor peak power. Approximately one and a half hours elapsed between bursts to allow the reactor to cool. Thus, a graph such as that of mercury pressure variation shown in the next chapter took more than a day to produce.

IV. EXPERIMENTAL FINDINGS

A description of the first direct nuclear pumped laser to operate in the visible light range will be presented here. This will be preceded by a summary of the gain measurements that led to the laser's discovery.

A. Description of Unblocked/Blocked Measurements

Using the laser described in Chapter III, the ratios shown in Fig. 12 were measured. Comparatively large light output for the 6150-Å line was observed with the back mirror unblocked while less light was observed with it blocked.

An approximate value for the actual percentage of gain per unit length represented by these ratios can be arrived at.[42] However, experimental variations in window loss, mirror loss, alignment and geometry preclude an absolute calibration. Nevertheless, there is a relationship between a given ratio and gain for a given set of experimental conditions and the ratios may be used as predictors for optimum lasing conditions.

Figure 13 shows ratios measured with the laser operating electrically. It can be seen that as the input power (and current) increases, the ratios also increase. When the input power reaches a critical point, the ratios become extremely large, and lasing commences. By measuring the change in ratios below this critical point with variation of mercury and helium pressure, it is possible to optimize these parameters.

The 6150-Å ratios are compared to 6560-Å ratios in Fig. 12 to show an absolute indication of gain. A population inversion is not expected for either the 6560-Å helium-ion transition, or the 6563-Å hydrogen-ion transition, the two possible components of the signal displayed. However, due to the fast radiative decay of the lower state for each of these

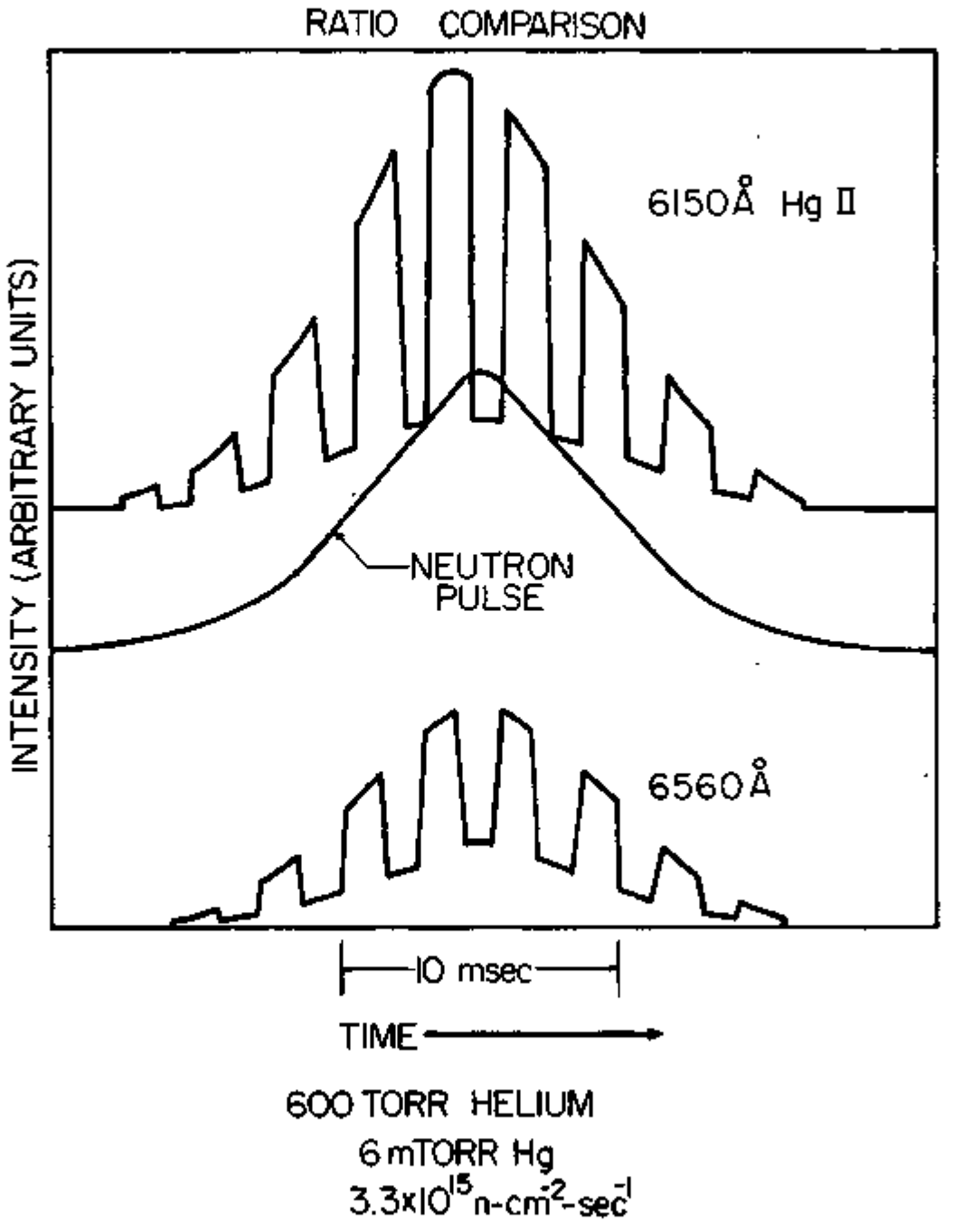

Fig. 9. 6150-Å ratios are compared to 6560-Å ratios to show an absolute indication of gain.

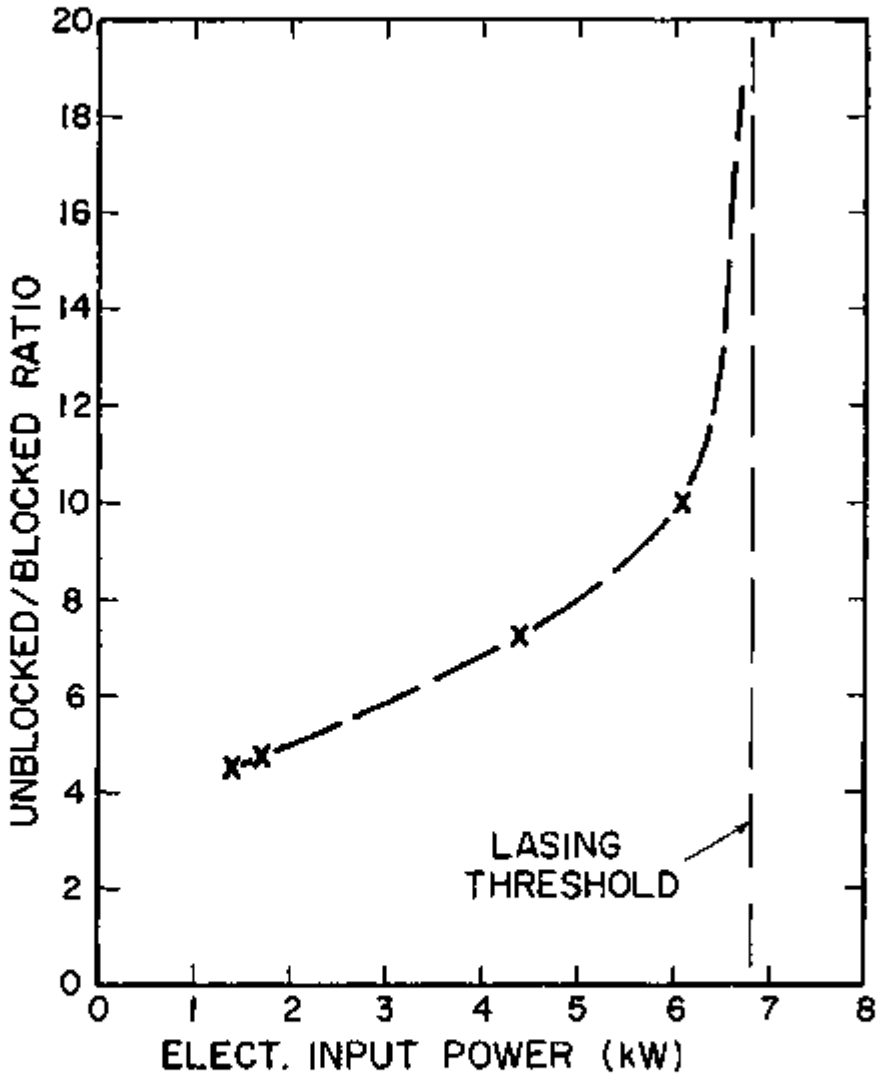

Fig. 10. Ratios measured with the laser operating electrically. When input power reaches the laser threshold, the ratios become extremely large and lasing commences.

transitions,[43,44] the amount of absorption is expected to be less than 0.01% for the 60-cm active length used here. In addition, these transitions are well within the bandwidth of the dielectric mirrors.

Just as a lower limit to the gain may be set by comparison to a line exhibiting minimal absorption, an upper limit may also be arrived at. Adding up the cavity losses one arrives at a 4% to 6% loss per pass. This is an upper limit on the single pass gain, since a higher gain would allow lasing to occur.

Figures 14 and 15 show the variation of ratios with total pressure and mercury pressure. One can compare these with the laser performance graphs in section B2 of this chapter and see that these predict closely the conditions under which lasing was discovered. In Fig. 14 a broad maximum occurs at around 600 Torr total pressure, while Fig. 15 shows a peak value at around 3.5 mTorr.

The graph of ratios vs. mercury pressure demonstrates yet another point. The essential difference between the lasers used to acquire these curves was that a one meter radius of curvature mirror instead of a five meter radius of curvature mirror was used at the rear of the cavity for the lower set of ratios. The cavity length was 98 cm. Hence, window losses and mirror reflectivities are not the only important factors in determining how well a given laser cavity will perform. In this case the shorter radius of curvature introduces additional light losses within the cavity, thus lowering the ratios.

More information may be extracted by measuring the unblocked/blocked ratios as a function of neutron flux for a given nuclear reactor pulse. In Fig. 16 the ratios remain fairly constant for the 6560-Å light, while they increase with higher neutron flux for the 6150-Å light. The top

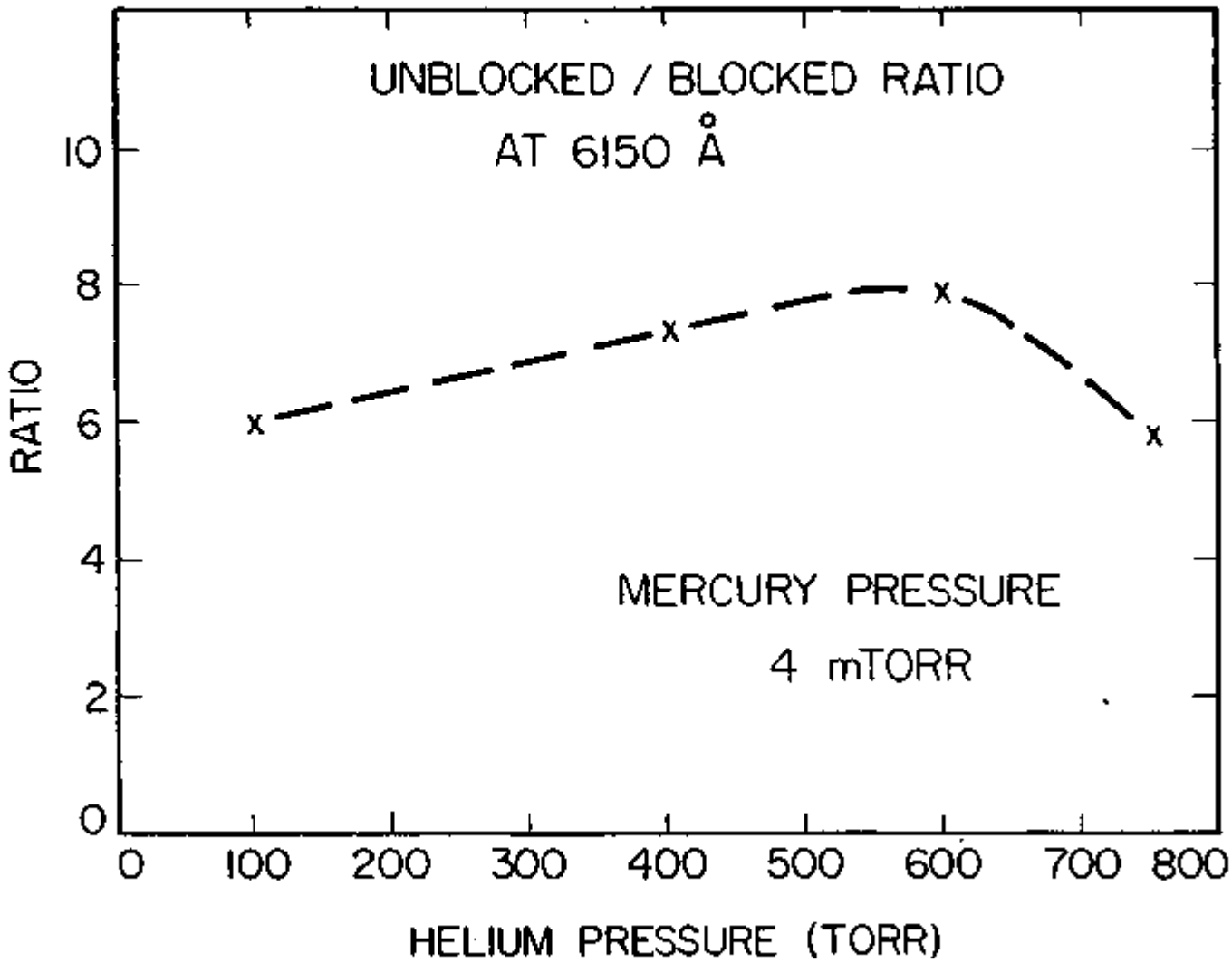

Fig. 11. Variation of ratios with total pressure, showing a broad maximum ~600 Torr total pressure.

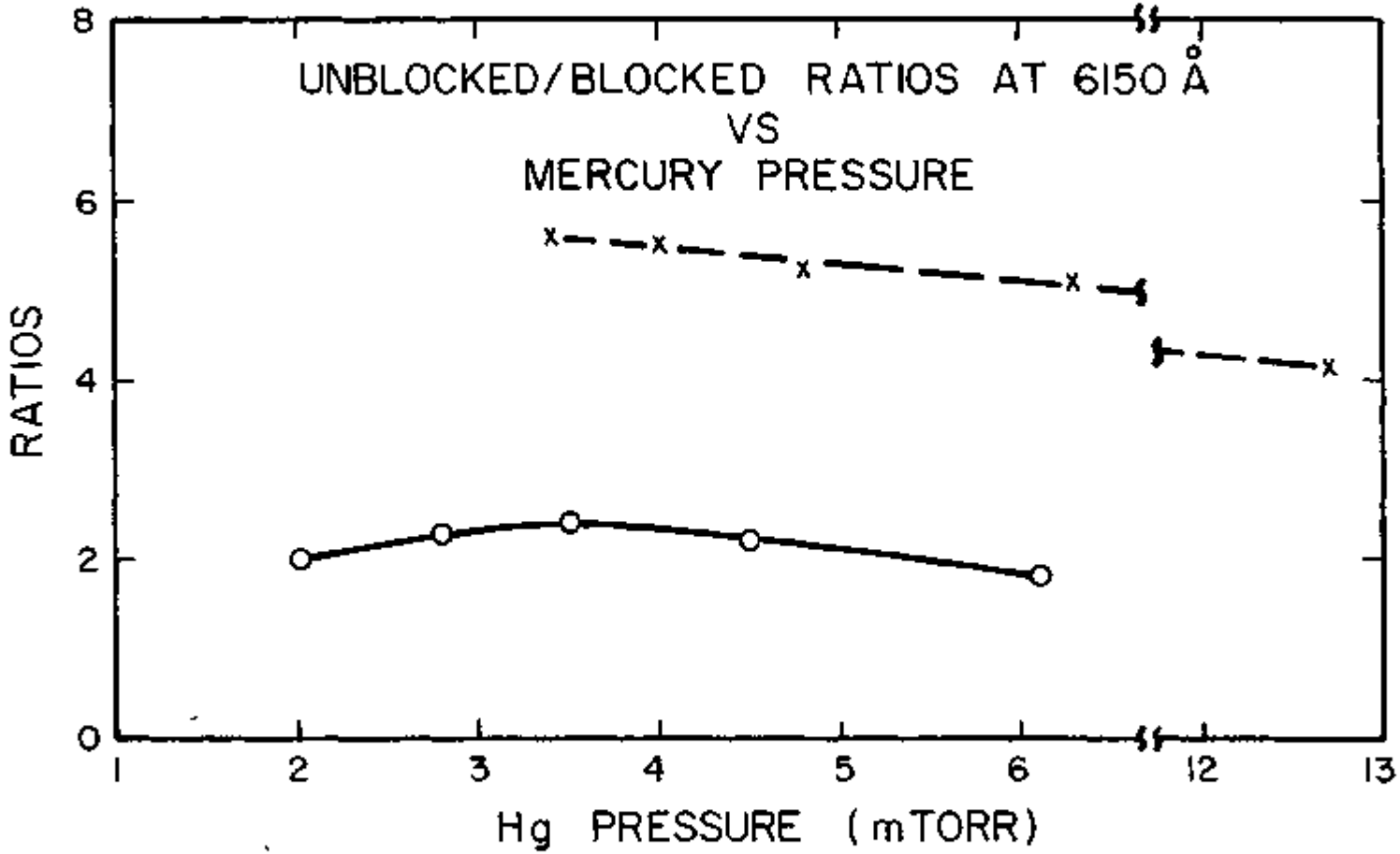

Fig. 12. Variation of ratios with mercury pressure, indicating a peak value at ~3.5 mTorr.

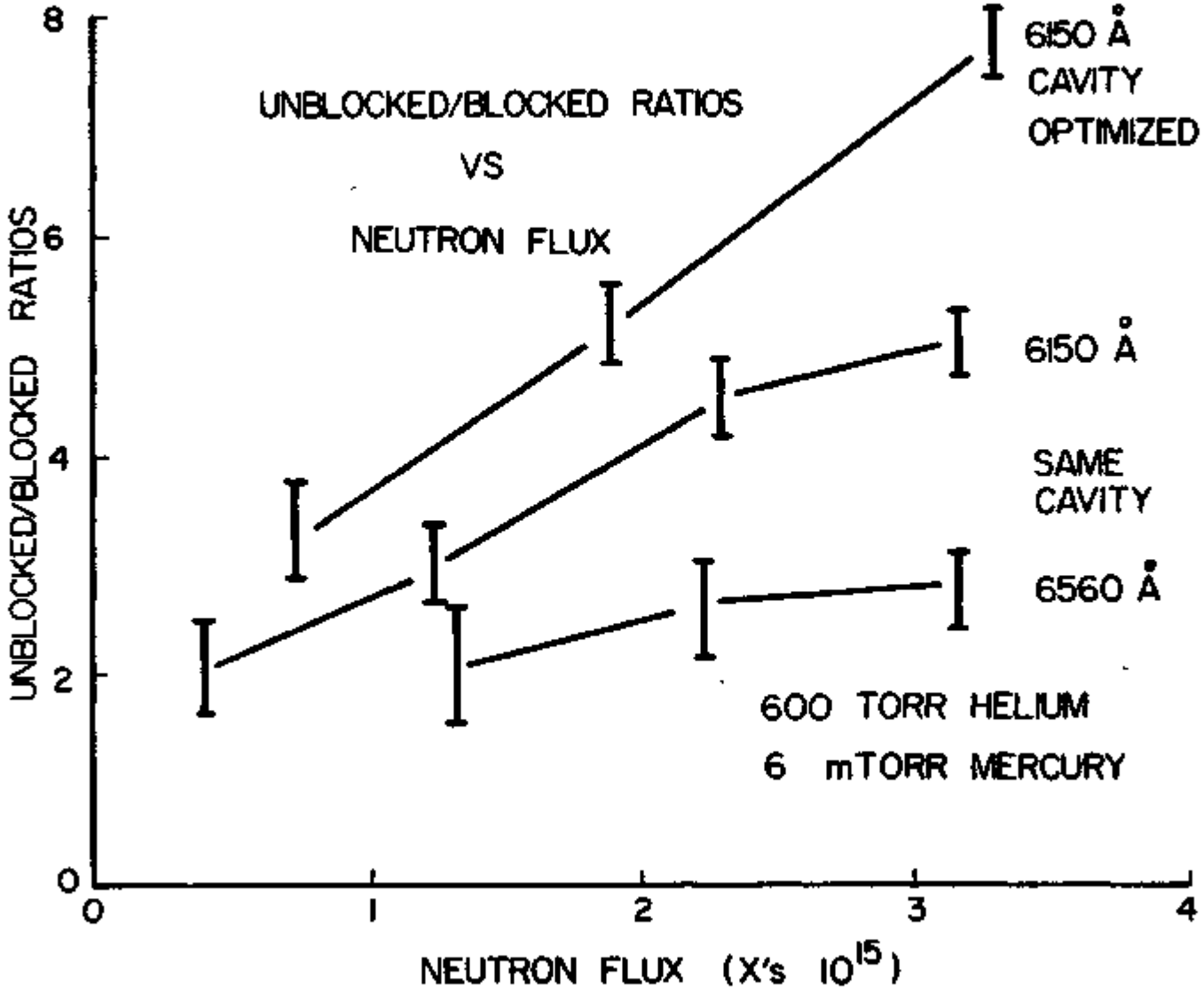

Fig. 13. Variation of unblocked/blocked ratios as a function of neutron flux. The ratios remain fairly constant for 6560-Å light, while they increase with higher neutron flux for the 6150-Å light.

curve indicates a linear increase in ratios with flux. This builds yet a better case for the argument that a higher neutron flux will increase the gain to the laser threshold.

The blocked signal intensity at peak neutron flux was graphed for a group of pulses taken under identical conditions, but with the pressures varying as shown in Fig. 17. The cross over at intermediate total pressures was unexpected. The possible error in any given measurement ranges from approximately ±25% at low helium pressure to ±15% at high helium pressure.

In the next section, the description of the discovery of a laser at 6150-Å that employs these experimental conditions shows that the prediction was good.

B. Nuclear Laser Experiment at Sandia

The laser was set up and aligned as described in Chapter III. Lasing was demonstrated by blocking the back mirror. This reduced the signal strength to values characteristic of the radiation induced background noise. Therefore, large light signals observed with the back mirror unblocked are completely the result of the high reflectivity mirrors at the ends of the laser cavity, and their alignment. When the laser output is plotted as a function of neutron flux, a threshold of approximately 1×10^{16} n/cm^2-sec is indicated.

The laser was operated electrically at low pressure so as to produce the same photomultiplier output as during nuclear reactor operation. Sighting along the laser axis, a red spot approximately 0.75-cm across was clearly discerned. Upon blocking the back mirror no spot was observed and the 6150-Å light reaching the photomultiplier was too small to be measured. Hence, the signal strengths measured during nuclear reactor

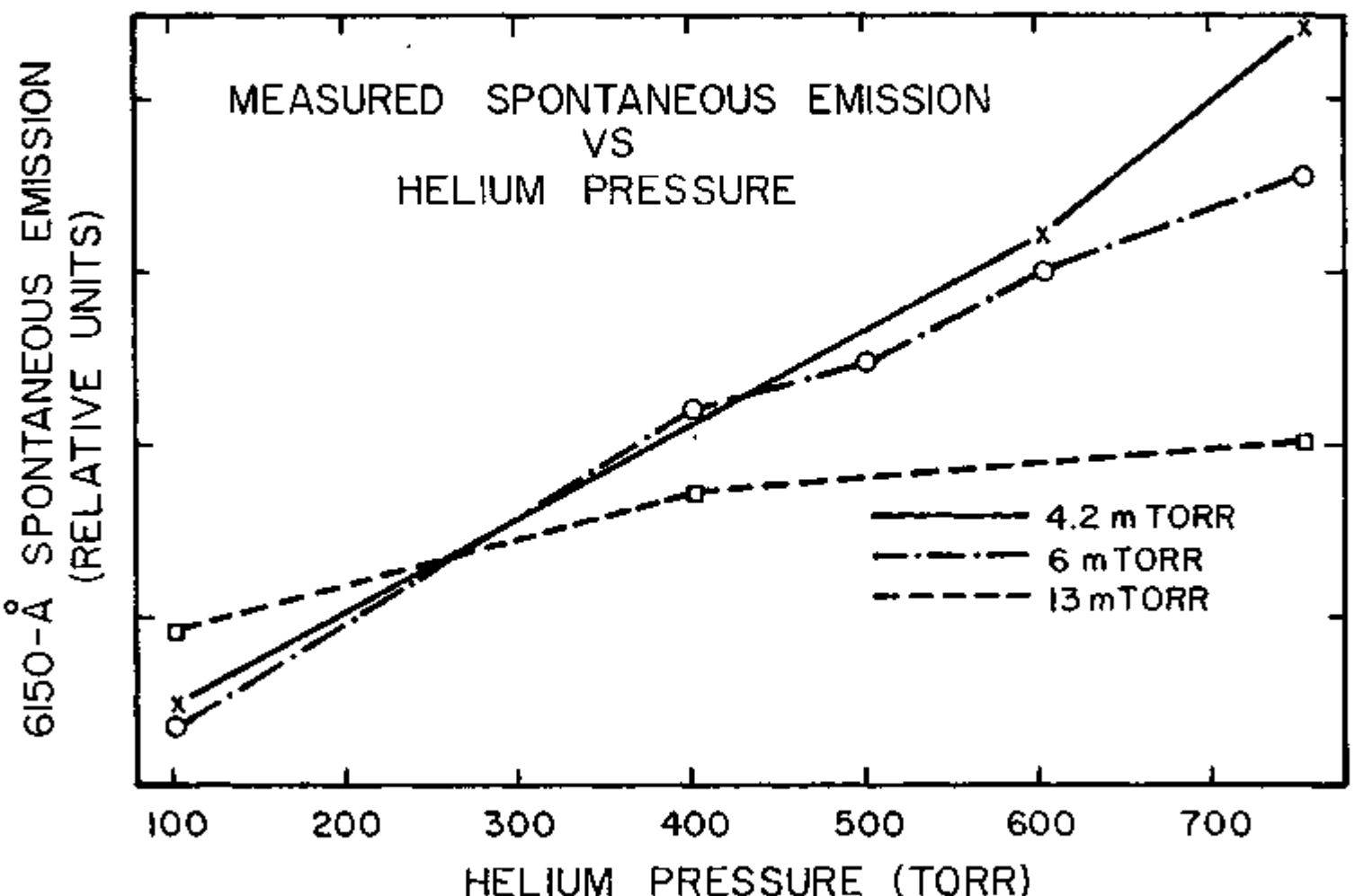

Fig. 14. The blocked signal intensity at peak neutron flux was graphed for a group of pulses taken under identical conditions.

operation were completely consistent with electrical lasing characteristics.

Finally, lasing occurred for helium and mercury pressures predicted by gain measurements at the University of Illinois TRIGA reactor, and with a threshold about twice the neutron flux available at Illinois.

A power meter and a nominal 4 mW helium-neon 6328-Å alignment laser were used to estimate the nuclear laser output. The peak nuclear laser output corresponded to a power of ~1 mW. This measurement led to an efficiency of 10^{-6}%, based on a calculated 90 kW peak power deposited in the gas during nuclear reactor operation.

The laser was not optimized for maximum output. It is possible that the mirror alignment could have been improved or window losses reduced. The 1% transmission output coupler could have been replaced with a larger transmission mirror to improve output. In addition, a measurement of the actual power deposited in the gas with the ^{10}B coating used in the laser could be lower than the somewhat idealized calculated value. The upper state densities estimated in Chapt. 2 lead to an efficiency of ~0.5%, somewhat lower than the quantum efficiency of 8%.

1. Proof of Lasing

Figures 18, 19 and 20 display a set of oscilloscope traces demonstrating that lasing occurred. In Fig. 18, the total laser output for optimum conditions is shown. One may compare the traces in Fig. 18 and see that the light output is coincident with the thermal neutron flux.

Figure 19 shows the photomultiplier output with the back mirror blocked. A smaller amount of light would be expected since multiple reflections within the cavity can no longer occur. When one observes the signal, there is not only a decrease in signal strength, but also a

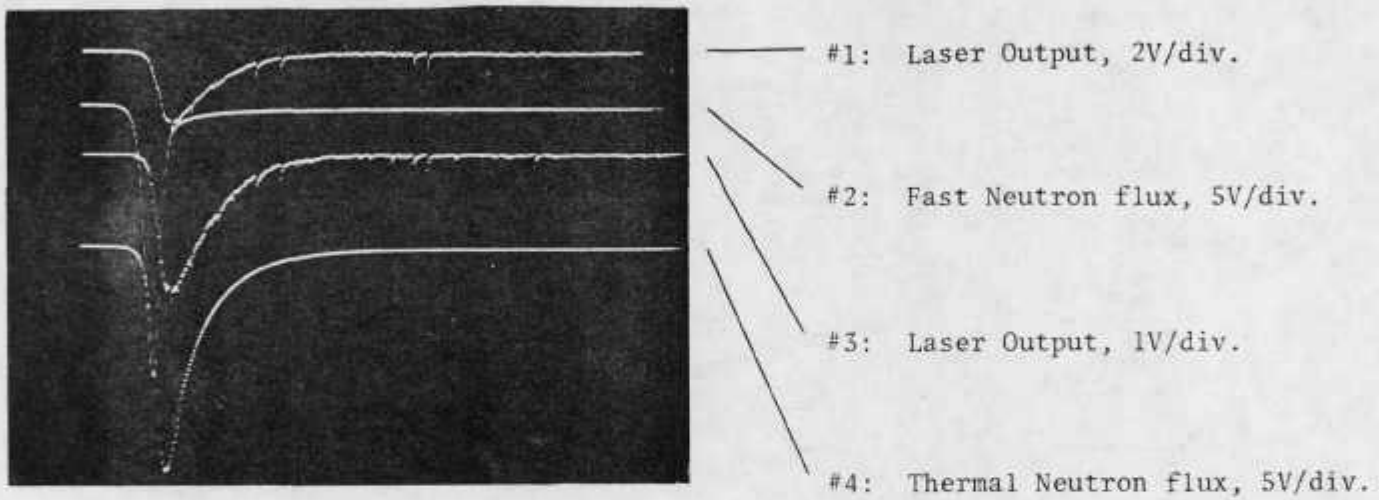

Fig. 15. Oscilloscope traces showing the total laser output for optimum pressures and $5.8 \times 10^{16} n/cm^2$-sec thermal neutron flux. The light output is coincident with the thermal neutron flux.

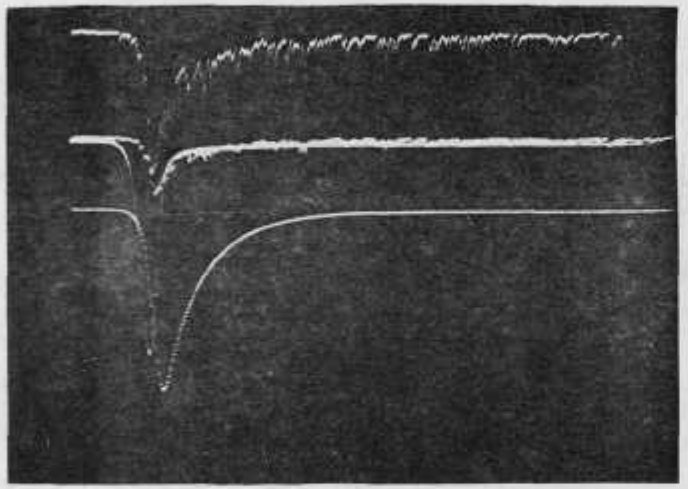

Fig. 16. Oscilloscope traces with the back mirror blocked and $4.7 \times 10^{16} n/cm^2$-sec thermal neutron flux. There is not only a large decrease in signal strength but a shift to the left of the signal peak with respect to the peak of the thermal neutron flux.

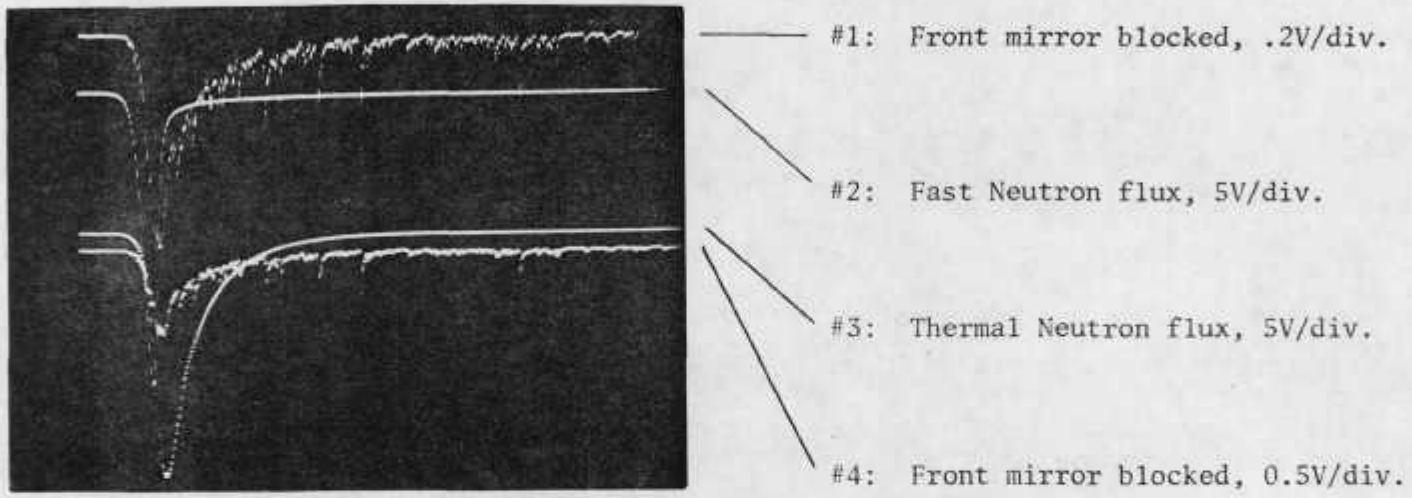

Fig. 17. Oscilloscope traces with the output mirror of the laser blocked and 6×10^{16} n/cm^2-sec thermal neutron flux. No light from the laser was allowed to reach the detector. The same temporal behavior was observed as for Fig. 19.

shift to the left of the signal peak, i.e. more nearly in phase with the fast neutron burst (and associated noise) than with thermal neutrons.

Time is displayed on the horizontal axis, with zero set at the peak of the thermal flux. Hence, a shift to the left indicates that the event takes place earlier in time. The resultant signal must be compared to the traces in Fig. 20. For this burst, the output mirror of the laser was blocked, thus allowing no light from the laser to reach the detector. The same temporal behavior was observed as for Fig. 19 and the signals were roughly equivalent when one allowed for the variation in peak neutron fluxes for the two bursts. Hence, the light emitted with the back mirrors blocked is too weak to be observed above the noise.

The radiation noise that composes Fig. 20 appears to have two components. First, there is a uniform envelope following the time response of the fast burst. Second, there are random peaks distributed over the trace up to 0.5V in height, and several microseconds wide. Increasing the lead shielding thickness decreased the amount of noise, indicating radiation coming through the shielding was the cause of much of this noise. In addition, the spikes are fairly well confined to the fast burst time scale, when the rate of neutron and gamma formation is greatest. Electrical pickup also could have been a source of noise. It is the random nature of the radiation noise that introduces the largest error in evaluating the data. Three noise signals were measured carefully and graphed as shown in Fig. 21. However, the data were first normalized to a peak thermal neutron flux of $1.95 \times 10^{16} n/cm^2$-sec.

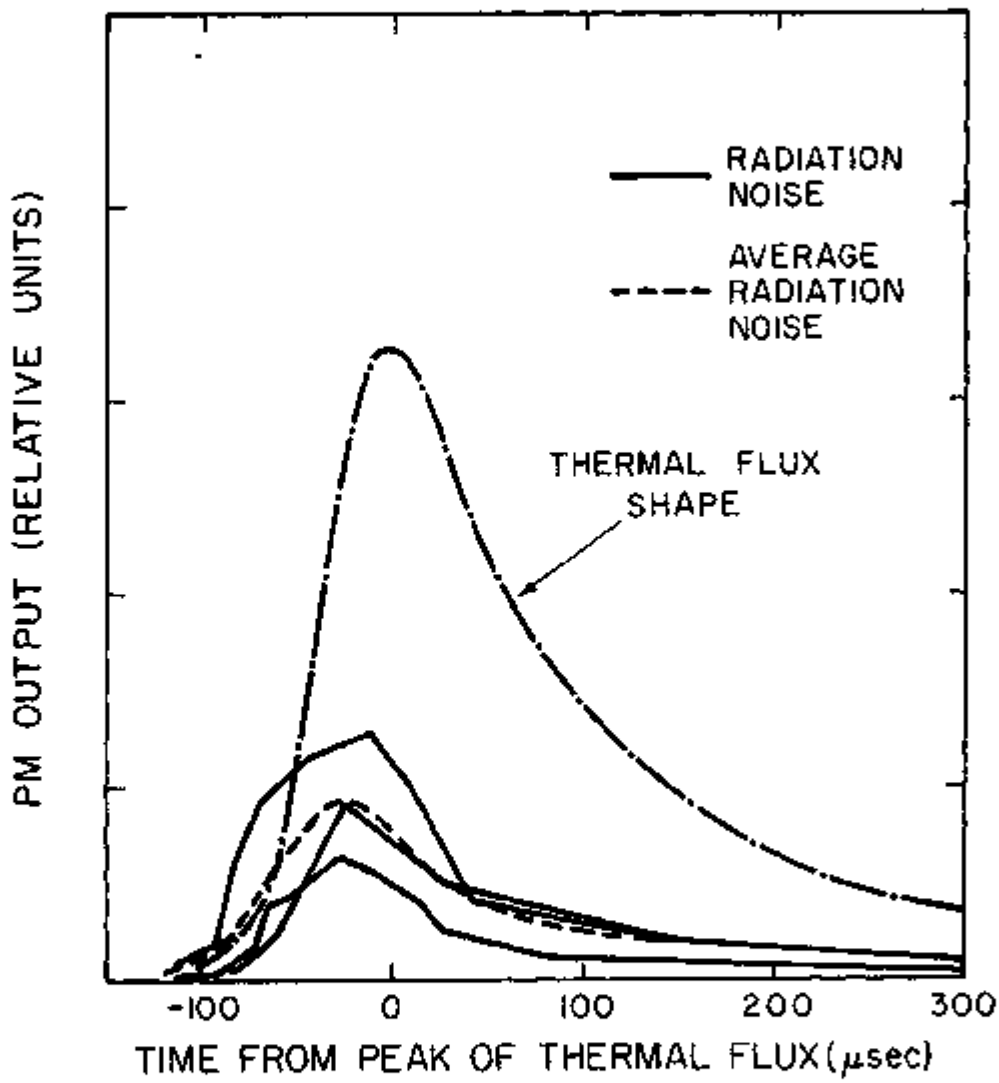

Fig. 18. Three noise traces were measured and graphed. An average radiation noise level was plotted. Random radiation noise is not shown.

An average noise signal, shown as a dashed line in Fig. 21, was constructed from the three noise signals and subtracted from each laser signal to arrive at the shape of the laser output. Two bursts were taken with the back mirror blocked, and the data derived from these are shown with the average noise in Fig. 22. It can be seen that there is no measurable light signal above background when the back mirror is blocked. The difference in magnitude between the three traces is attributed to the random nature of the noise.

Figure 23 allows a direct comparison between the total laser output, the noise, and the back mirror blocked signal. The measured maximum and minimum values for the noise are indicated by the error bars. The random spikes have been smoothed out, as in Figs. 21 and 22. The time delays already mentioned may be seen here, as well as the large signal variation, proving that lasing occurred. In addition, it appears that the laser is operating steady state, i.e. it operates throughout the thermal neutron pulse.

Figure 24 displays the signal intensity as a function of thermal neutron flux for several bursts. Two points at the optimum mercury pressure of 2.5 mTorr indicate a threshold for lasing of 1.3×10^{16} n/cm^2-sec, while three points taken between 6 and 10 mTorr indicate a threshold of 1.9×10^{16} n/cm^2-sec.

The threshold measurement at 2.5 mTorr was attempted on the last day of pulsing. A flux of 3×10^{16} n/cm^2-sec was requested, and the reactor output reached 5.4×10^{16} n/cm^2-sec instead, making a good measurement out of the question. This amount of variation was typical during the 8 days allowed for the experiment. These thresholds are consistent with the fact that the laser did not work at the University of Illinois with

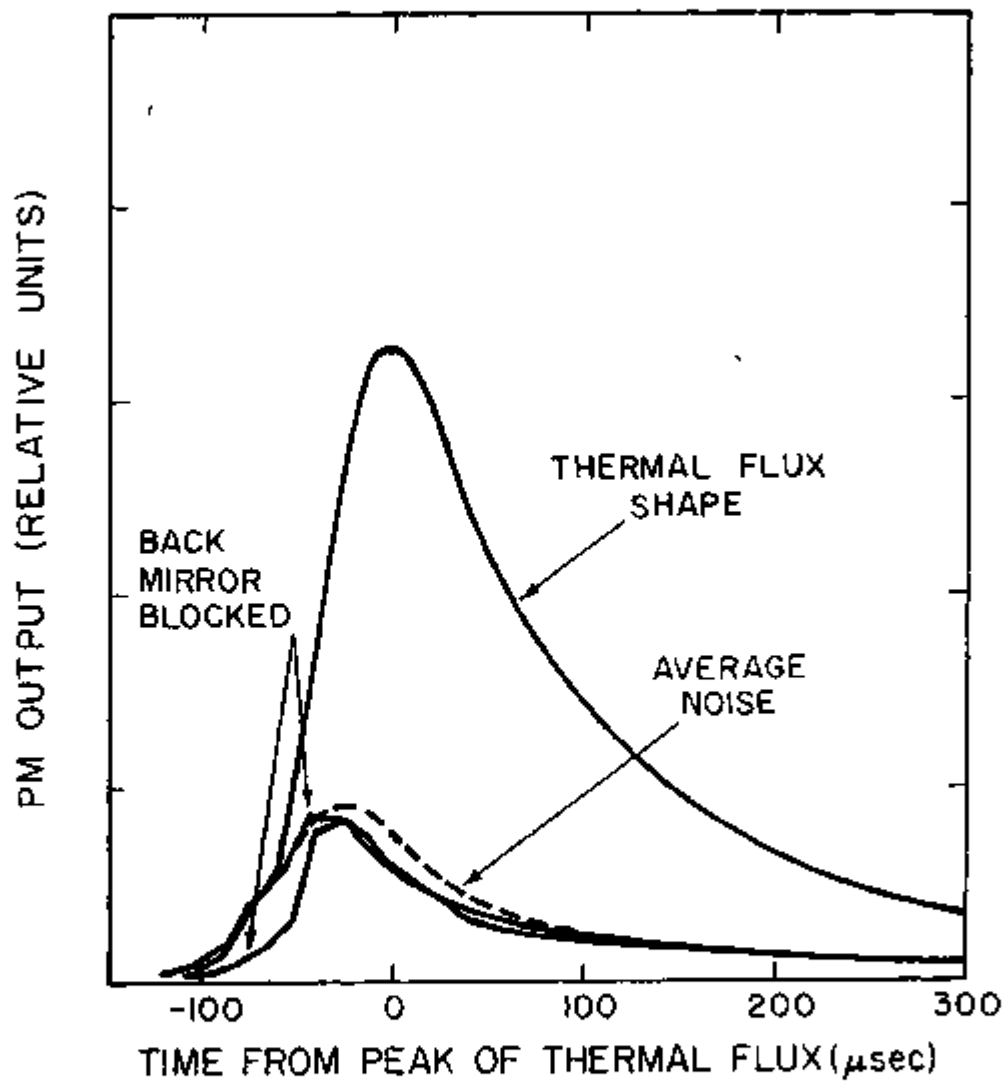

Fig. 19. The back mirror was blocked for two bursts and the data are shown with the average noise.

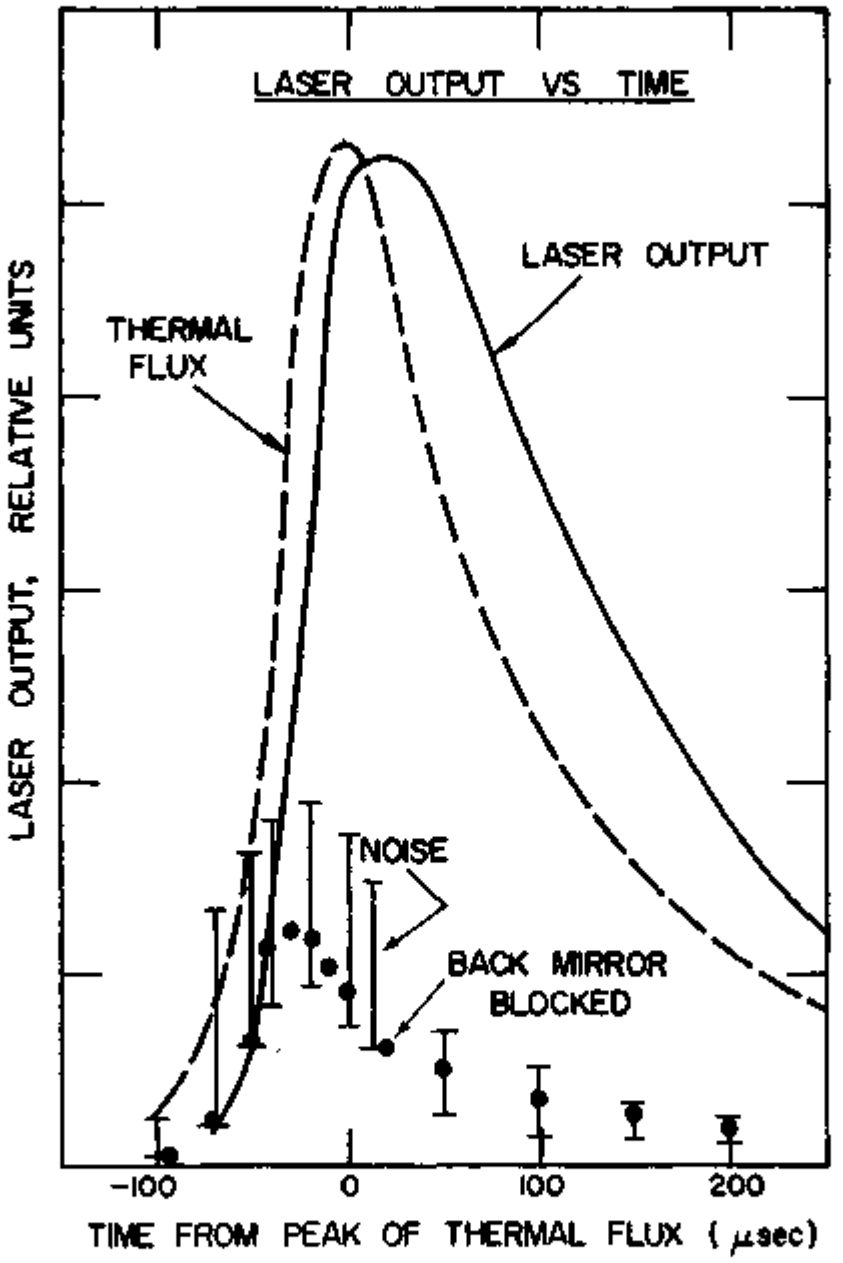

Fig. 20. A graph comparing directly the total laser output, the noise and the back mirror blocked signal. The measured maximum and minimum values for the noise are indicated by the error bars.

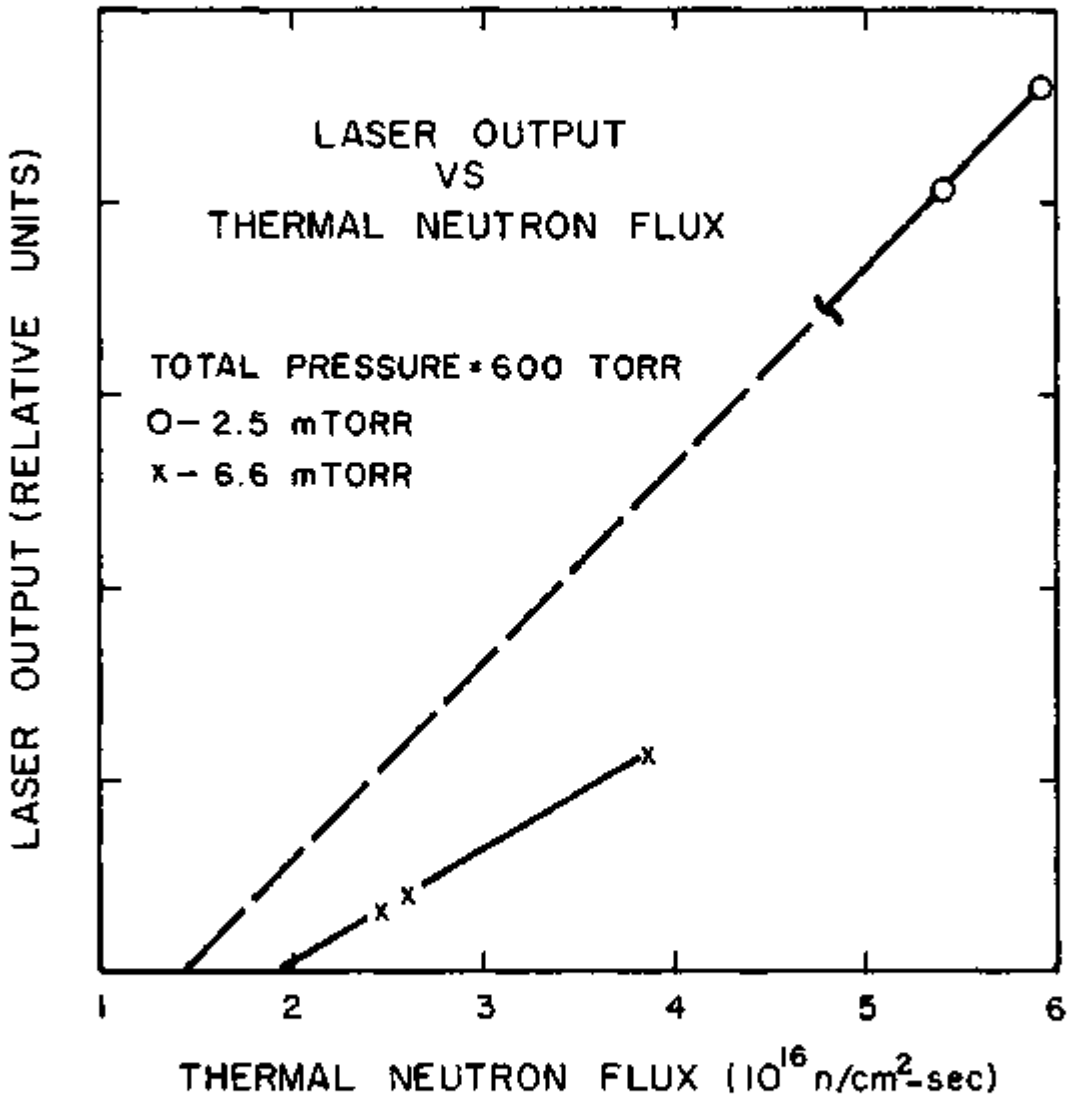

Fig. 21. Laser output as a function of thermal neutron flux.

neutron fluxes up to $5x10^{15}n/cm^2$-sec. They indicate that increased gain resulting from the increased neutron flux allowed lasing to occur.

2. Pressure Variation

The mercury vapor pressure was varied in eight bursts between 2 and 10.2 mTorr. As shown in Fig. 25, the output increases as the mercury partial pressure is reduced, although this effect appears to begin saturating at ~2.5 mTorr. The measurements were made at peak thermal neutron fluxes varying from $2.5x10^{16}n/cm^2$-sec to $4.8x10^{16}n/cm^2$-sec due to natural variation in nuclear reactor operation. Therefore, all points have been adjusted to an intermediate value of $3.8x10^{16}n/cm^2$-sec.

The gain measurements shown in Fig. 15 indicate a peak around 3.5 mTorr mercury partial pressure. This is consistent with the apparent turnover in laser output at 2.5 mTorr. The uncertainty in temperature measured for the two different experiments could easily account for the apparent shift in mercury partial pressure.

A single nuclear reactor pulse at a total pressure of 300 Torr yielded a laser output 40% lower than at 600 Torr. This trend is consistent with gain measurements shown in Fig. 14. Time did not allow a complete pressure survey.

3. Duplication of V. M. Andriakhin's Experiment

In addition to the experiments just described, an attempt was made to achieve lasing with the same experimental conditions of flux and pressure used by V. M. Andriakhin in a previous experiment.[10]

Table 3 was prepared to allow easy comparison between the known features of Andriakhin's helium-mercury experiment and the present helium-mercury experiment.

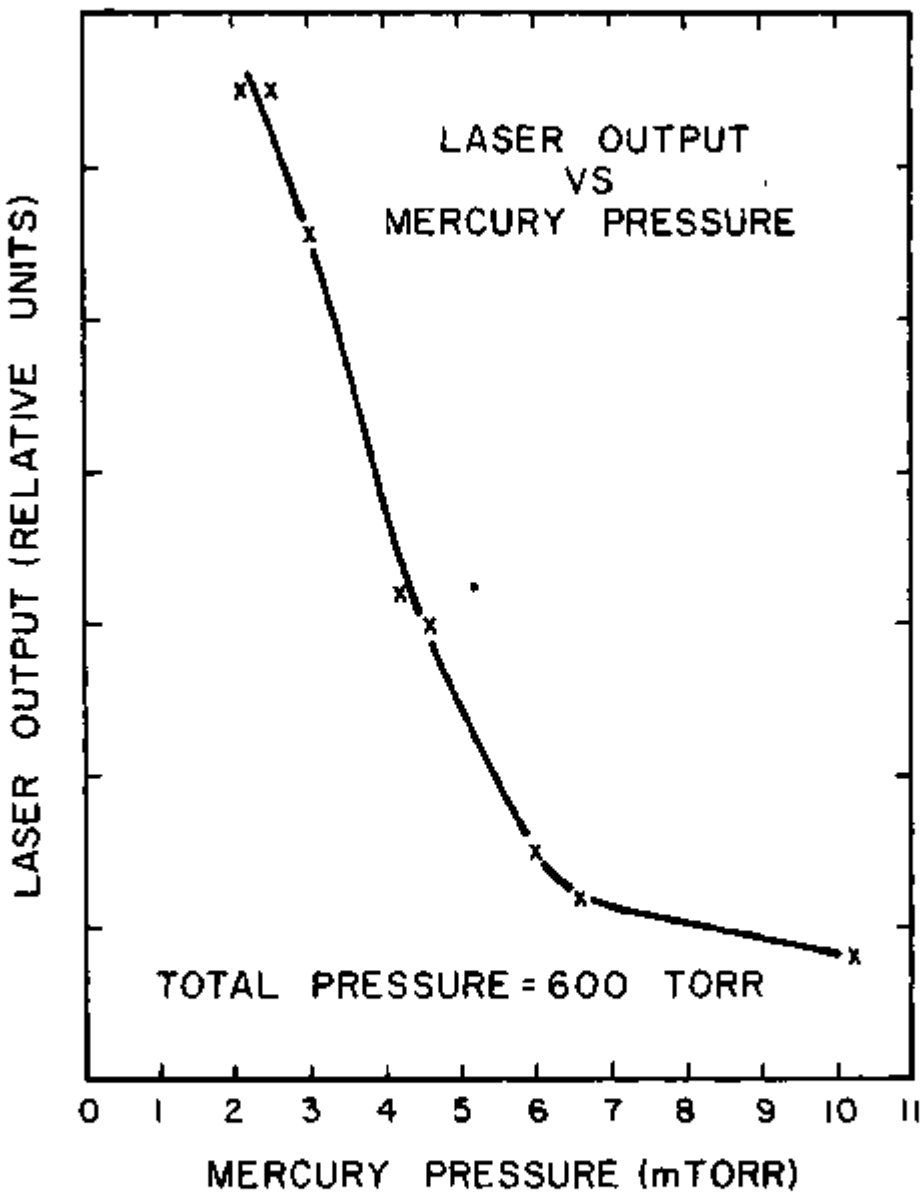

Fig. 22. Laser output as a function of mercury partial pressure.

	Moscow State University	University of Illinois
Active Volume Dimensions		
Length:	60 cm	60 cm
Diameter:	4 cm	2.4 cm
Mirrors		
Back:	R ~ 88%* (gold on Pyroceram)	R=99.9% at 6150 Å (dielectric on high purity fused quartz)
Output:	R=98% at 6328 Å (dielectric on glass)	R=99% at 6150 Å (dielectric on high purity fused quartz)
Temperature	150°C	150°C at reservoir**
Total Pressure	350 Torr	350 Torr***
Energy Producing Reaction	$n(He^3,P)T$	$n(B^{10},\alpha)_3Li^7$
Thermal Neutron Flux	$\sim 5\times10^{16}$ n/cm^2-sec	$>6\times10^{16}$ n/cm^2-sec
Peak Power Deposited in Laser	1.5×10^5 watts	1.5×10^5 watts

Table 3. A Comparison of Known Features of Andriakhin's Experiment and the Present Nuclear Laser

*Estimated R = 88% based on Table of Reflectivity of Gold vs. Wavelength.[45]

**The Illinois laser tube was 153°C over the middle 60 cm section and 162°C at the ends to prevent mercury from plating out on optical surfaces. A side arm was maintained at 150°C.

***It was assumed that 350 Torr was introduced before the tube was heated.

The dimensions of Andriakhin's laser were such that the volume was 754 cm^3. This compares with 271 cm^3 for the University of Illinois laser. The Soviet back mirror was a gold film, for which the reflectivity must have been approximately 88% or less.[45] A value of 99.9% was measured for the University of Illinois laser. The temperatures were the same, but it is not known whether the Soviets filled their laser before heating, or after heating. It was assumed that the 350 Torr pressure measurement was made before heating the laser, since this would lead to a more favorable energy deposition. The thermal flux measurement for the University of Illinois experiment is an underestimate since it was made at one end of the polyethylene, away from the peak neutron flux region. The peak power deposited in the gas as listed in the table was ascertained from Fig. 1.

The power deposited per unit volume is 2.5 times higher in the University of Illinois experiment than in the Moscow State University experiment.

No indication of light output was observed above the noise when Andriakhin's experiment was duplicated. Figure 26 shows the comparison of the output to the average noise. The thermal neutron flux is also shown for comparison of the time response. It is apparent that this "signal" is indistinguishable from the noise.

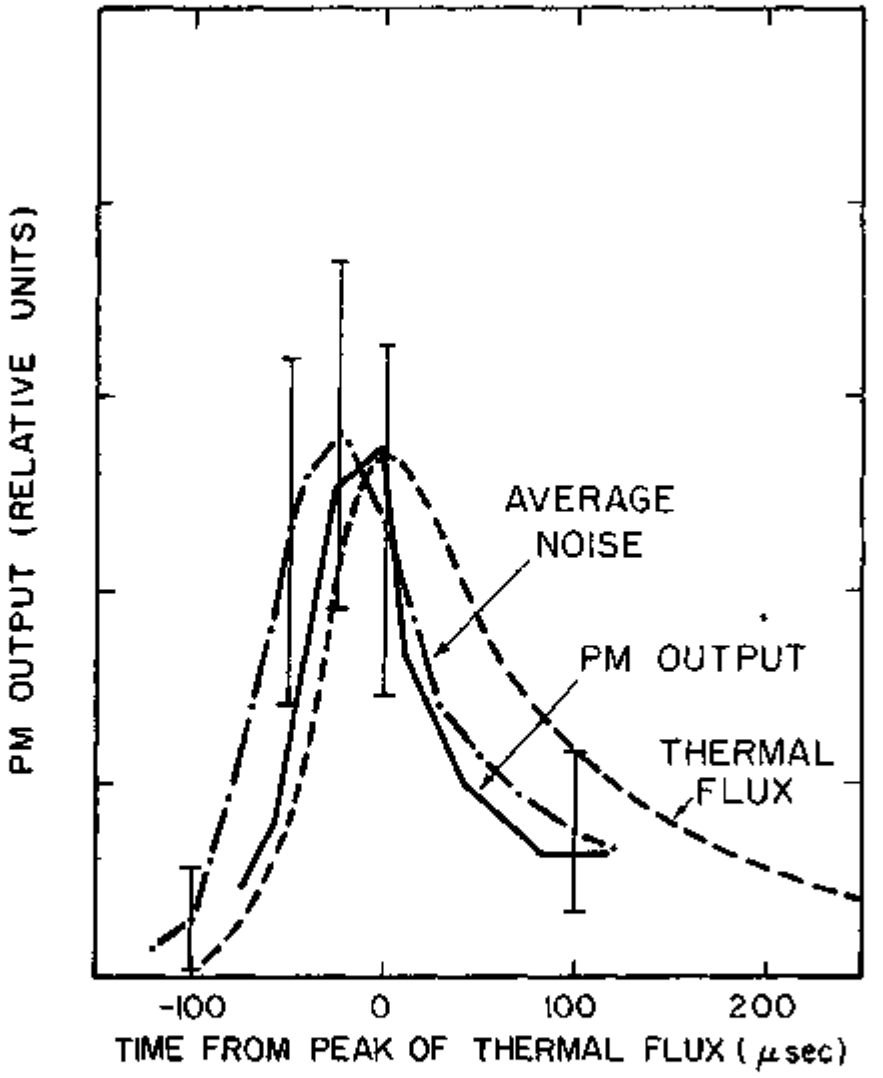

Fig. 23. In duplicating Andriakhin's experiment, the light output could not be distinguished from the noise. This graph compares the output to the average noise.

V. CONCLUSIONS AND SUGGESTIONS FOR FURTHER RESEARCH

A. Conclusions

The task of this research, stated simply, was to produce a direct nuclear pumped laser in a helium-mercury mixture. This has been done using the SPRII reactor at Sandia Laboratories. The laser utilized the $^{10}B(n,\alpha)^{7}Li$ nuclear reaction to excite the gas, with thermal neutron fluxes up to $5.8 \times 10^{16} n/cm^2$-sec.

The thermal neutron flux threshold for lasing was $\sim 10^{16} n/cm^2$-sec, and the peak power output ~1 mW at 6150 Å. This results in an efficiency of $\sim 1 \times 10^{-6}$%, somewhat lower than typical electrical lasing efficiency. With further optimization it may be possible to improve this efficiency. Further, the 400μsec laser output indicates steady state operation.

In addition to the laser experiments, gain measurements have been made using a similar experimental arrangement, but with a thermal neutron flux too low to produce lasing. These measurements successfully predicted the operating regime of the DNPL and the Sandia Laboratory reactor's large neutron flux made its discovery possible.

Some questions remain unanswered. But these questions were not even conceived of at the beginning of this research. The one central question all along was, "Is a DNPL in a helium-mercury mixture possible?"

This question has been answered.

B. Suggestions for Further Work

The present study has uncovered several DNPL possibilities in addition to the 6150-Å mercury-ion line reported here.

The $7^2P_{1/2}$ - $7^2S_{1/2}$ transition shows many similarities to the $7^2P_{3/2}$ - $7^2S_{1/2}$ transition with electrical excitation and should provide a nuclear laser that behaves almost identically to the $7^2P_{3/2}$ - $7^2S_{1/2}$ DNPL.

Population inversions may also be possible for the $7^2S_{1/2}$ - $6^2P_{3/2}$ and the $7^2S_{1/2}$ - $6^2P_{1/2}$ transitions, also in the mercury ion. These transitions have wavelengths of 2848 Å and 2260 Å, respectively. The calculated upper state lifetimes are longer than the lower state lifetimes, indicating possible steady state lasing.[40]

In addition to these mercury-ion possibilities, there are at least two candidates in neutral mercury. The $6P^3P_2$ - 7^3S transition at 1.53μ has been observed electrically in the lasers described here and has exhibited very high gain. Lasing was observed during this research at Sandia using mirrors highly reflective at 1.50 μm ± 10% in a second ^{10}B powered helium-mercury laser. It is possible that this lasing was at 1.53 μm, though lasing was not consistent enough from one pulse to the next to make a positive identification possible.

The 7^3S - 6^3P_2 transition may also be capable of population inversion. Since the lower level is a metastable, one would not expect this to lase, except perhaps in a short, fast rise time pulse. However, recent experiments at the University of Illinois Gaseous Electronics Laboratory show that optical gain is possible for a helium-mercury mixture with mercury pressures greater than 10 Torr and total pressures from 50 to 150 Torr with electrical excitation.[46]

In Chapter II the reaction:

$$He^*(2^3S) + Hg^*(6^3P_0) \rightarrow Hg^*(7^2P_{3/2}) + He + e^- \qquad \text{(II-2)}$$

was proposed as a possible populating mechanism for the $7^2P_{3/2}$ level

at high total pressure. An absorption experiment could be performed at the University of Illinois TRIGA reactor to measure the metastable densities as a function of helium and mercury pressure. Then the light intensity at 6150 Å should be proportional to the product of the $Hg^*(6^3P_0)$ and $He^*(2^3S)$ metastables if the process is dominant.

Also in Chapter II, the reaction

$$He_2^+ + Hg \rightarrow Hg^+ (7^2S_{1/2}) + 2He \qquad \text{(II-12)}$$

was proposed as a populating mechanism for the $7^2S_{1/2}$ level in the helium-mercury 6150-Å DNPL. Photographs taken of the helium-mercury spectrum during reactor operation also indicate that the $7^2S_{1/2}$ level is not populated solely by radiative transitions from the $7^2P_{3/2}$ level.

A study that would identify in a definitive manner whether or not the helium molecular ion is responsible for this variation and that would measure the cross section for charge exchange would be valuable.

In addition to these specific suggestions, an eye should be kept on the ultimate goals for DNPLs. Promising lasers should be scaled to show the feasibility of high-power and high-pressure operation.

LIST OF REFERENCES

1. D. A. McArthur and P. B. Tollefsrud, "Observation of Laser Action in CO Gas Excited Only by Fission Fragments," *Appl. Phys. Letters, 26*, p. 181 (1974).

2. H. H. Helmick, J. L. Fuller and R. T. Schneider, "Direct Nuclear Pumping of a Helium-Xenon Laser," *Appl. Phys. Letters, 26*, p. 327 (1975).

3. R. J. DeYoung, W. E. Wells, G. H. Miley and J. T. Verdeyen, "Direct Nuclear Pumping of an Ne-N_2 Laser," *Appl. Phys. Letters, 28*, p. 519 (1976).

4. N. W. Jalufka, R. J. DeYoung, F. Hohl and M. D. Williams, "A Nuclear Pumped $^3He(n,p)^3H$ Reaction," *Appl. Phys. Letters, 29*, p. 188 (1976).

5. J. C. Guyot, G. H. Miley, J. T. Verdeyen and T. Ganley, "On Gas Laser Pumping Via Nuclear Radiations," *Trans. of the Symp. of Research on Uranium Plasmas and Their Technological Application, NASA SP-236* (1970).

6. G. H. Miley, "Nuclear Radiation Effects on Gas Lasers," in *Laser Interactions*, (Schwarz and Hora, eds.), Plenum Press, pp. 43-57 (1972).

7. G. H. Miley, J. T. Verdeyen, T. Ganley, J. C. Guyot and P. E. Thiess, "Pumping and Enhancement of Gas Lasers via Ion Beams," *11th Symp. on Electron, Ion and Laser Beam Technology* (R.F.M. Thomley, ed.), San Francisco Press, Inc. (1971).

8. G. H. Miley, J. T. Verdeyen and W. E. Wells, "Direct Nuclear Pumped Lasers," *Proc. 28th Gaseous Electronics Conf., EB-1*, Univ. of MO at Rolla (1975).

9. K. Thom and R. T. Schneider, "Nuclear Pumped Gas Lasers," *AIAA Journal, 10*, p. 400 (1972).

10. V. M. Andriakhin, V. V. Vasil'nov, S. S. Krasil'nikov, V. D. Pis'mennyi and V. E. Khvostinov, "Radiation of Hg-He^3 Gas Mixture Bombarded by a Neutron Stream," *JETP Letters, 12*, p. 58 (1970).

11. G. H. Miley, W. E. Wells, M. A. Akerman and J. H. Anderson, "Recent Nuclear Pumped Laser Results," *The 3rd Conf. on Partially Ionized Plasmas*, Princeton University, Princeton, N.J. (1976).

12. M. A. Akerman, G. H. Miley and D. A. McArthur, "A Direct Nuclear Pumped He-Hg Laser," *Appl. Phys. Letters*, to be published (1976).

13. W. E. Bell, "Visible Laser Transitions in Hg^+," *Appl. Phys. Letters, 4*, p. 34 (1964).

14. R. A. Myers, H. Wieder and R. V. Pole, "Wide Field Active Imaging," *IEEE J. Quant. Elect., QE-2,* p. 270 (1966).

15. H. Kano, T. Goto and S. Hatton, "CW Oscillation of Visible and Near-Infrared Hg(II) Lines in a He-Hg Positive Column Discharge," *J. Phys. Soc. Japan, 38,* p. 596 (1975).

16. V. S. Aleinikov, "Use of an Electron Gun to Determine the Nature of Collisions of the Second Kind in a Mercury-Helium Mixture," *Opt. Spect., 28,* p. 15 (1970).

17. H. Wieder, *et al.*, "Fabrication of Wide Bore Hollow Cathode Hg^+ Lasers," *Rev. Sci. Instr., 38,* p. 1538 (1967).

18. W. K. Schuebel, "Transverse-Discharge Slotted Hollow-Cathode Lasers," *IEEE J. Quant. Elect., QE-7,* p. 39 (1971).

19. A. L. Bloom, W. E. Bell and F. O. Lopez, "Laser Spectroscopy of a Pulsed Mercury-Helium Laser," *Phys. Rev., 135,* p. A578 (1964).

20. W. B. Bridges and A. N. Chester, "Spectroscopy of Ion Lasers," *IEEE J. Quant. Elect., QE-1,* p. 66 (1965).

21. I. M. Beterov, *et al.*, "Spectroscopic Properties of a Mercury Laser," *Opt. Spect., 27,* p. 208 (1969).

22. J. P. Goldsborough and A. L. Bloom, "Near-Infrared Operating Characteristics of the Mercury-Ion Laser," *IEEE J. Quant. Elect., QE-5,* p. 459 (1969).

23. E. Graham, IV, M. A. Biondi and R. Johnsen, "Spectroscopic Studies of the Charge-Transfer Reaction $He^+ + Hg \rightarrow He^+(Hg^+)^*$ at Thermal Energy," *Phys. Rev. A, 13,* p. 965 (1976).

24. H. Kano, *et al.*, "A Second Look at the Excitation Mechanism of the He-Hg^+ Laser," *Appl. Phys. Letters, 27,* p. 610 (1975).

25. I. P. Bogdanova, *et al.*, "Charge Exchange Between Helium Ions and Mercury Atoms," *Opt. Spect., 37,* p. 365 (1974).

26. J. A. Piper and C. E. Webb, "Power Limitations of the CW He-Hg Laser," *Opt. Comm., 13,* p. 122 (1975).

27. A. Ferrario, "Excitation Mechanism in Hg^+ Ion Laser," *Opt. Comm., 7,* p. 376 (1973).

28. D. J. Dyson, "Mechanism of Population Inversion at 6149 Å in the Mercury-Ion Laser," *Nature, 207,* p. 361 (1965).

29. N. Suzuki, "Spectroscopy of Mercury-Helium Discharge and 6150 Å Laser Oscillation," *Japanese J. Appl. Phys., 4,* p. 452 (1965).

30. R. J. DeYoung, M. A. Akerman, W. E. Wells and G. H. Miley, "Studies of Radiation-Induced Laser Plasmas," *1975 Int. Conf. on Plasma Science, 3D2*, Univ. of MI, Ann Arbor, MI, 75CH0987-8-NPS (1975).

31. M. A. Akerman, M. Konya, W. E. Wells and G. H. Miley, "Nuclear Radiation Enhancement of a Helium-Mercury Laser," *Trans. Am. Nucl. Soc.*, *22*, p. 133 (1975).

32. R. H. Lo and G. H. Miley, "Electron Energy Distributions in a Helium Plasma Created by Nuclear Radiations," *IEEE Trans. on Plasma Science, PS-2*, p. 198 (1974).

33. B. S. Wang, Ph.D. Thesis, University of Illinois (1972).

34. D. A. McArthur, "Development of the Fission-Fragment-Excited CO Laser Towards Higher Power," *The 3rd Conf. on Partially Ionized Plasmas*, Princeton University, Princeton, NJ (1976).

35. P. B. Lyons, J. S. Clarke and D. S. Metzger, "Gamma Initiated HF Laser," *IQEC-8*, San Francisco (1974).

36. P. J. Ebert, *et al.*, "Xenon Pumped by Gamma Rays," *IQEC-8*, San Francisco (1974).

37. J. C. Guyot, "Measurement of Atomic Metastable Densities in Noble Gas Plasmas Created by Nuclear Radiations," Ph.D. Thesis, University of Illinois (1971).

38. D. A. McArthur and P. B. Tollefsrud, "Measurement of Optical Gain in CO Gas Excited Only by Fission Fragments," *IEEE J. Quant. Elect.*, *QE-12*, p. 244 (1976).

39. R. J. DeYoung, W. E. Wells and G. H. Miley, "Optical Gain in a Neutron-Induced ^{3}He-Ne-O_2 Plasma," *Appl. Phys. Letters*, *23*, p. 194 (1976).

40. G. J. Collins, "Bates Damgaard Approximations of Hg II State Lifetimes," Private Communication (1975).

41. R. L. Byer, W. E. Bell, E. Hodges and A. L. Bloom, "Laser Emission in Ionized Mercury: Isotope Shift, Linewidth, and Precise Wavelength," *J. Opt. Soc. of Am.*, *55*, P. 1598 (1965).

42. C. B. Zarowin, M. Schiff and G. R. White, "The Use of Resonant Cavity Spectroscopy in Studying Populations in the He-Ne System," *Proceedings of the Symposium on Optical Masers, XIII*, p. 425 (1963).

43. W. L. Wiese, M. W. Smith and B. M. Gleanon, *Atomic Transition Probabilities Hydrogen through Neon*, NSRDS-NBS 4, *I*, p. 2 (1966).

44. A. L. Osherovich and Ya. F. Verolainen, "Lifetimes of the Levels of HeI and HeII," *Opt. and Spect.*, *24*, p. 81 (1968).

45. D. Röss, *Lasers Light Amplifiers and Oscillators*, Academic Press, p. 215 (1969).

46. J. K. Crane, B. E. Cherrington and J. T. Verdeyen, "Gain on the Mercury 5461 Å and 3650 Å in the Afterglow of a High Pressure Pulsed Discharge," *29th Gaseous Electronics Conf.*, Cleveland, OH (1976).

APPENDIX A

NUCLEAR RADIATION ENHANCEMENT OF A HELIUM-MERCURY LASER†

M. A. Akerman, M. Konya, W. E. Wells, and G. H. Miley

Significant nuclear radiation enhancement has been observed in a mercury vapor laser at 6150Å. Although previous enhancements have been reported by others[1] for infrared transitions in two other gases, this accomplishment with a mercury laser provides the first enhancement at a visible wavelength and the first enhancement of a laser operating by a charge exchange reaction[2]. These enhancements could be quite important in instances such as laser-fusion or laser isotope separation where optimum laser performance is mandatory.[3,4]

The laser was constructed from a pyrex tube 86 cm long, with high voltage electrodes at each end. The mercury vapor pressure was maintained in five torr He^3 by wrapping the laser with heating tapes. A temperature of 59°C in the laser produced a mercury partial pressure of 20 millitorr for this experiment. Dielectric mirrors, more than 99% reflective at 6150Å, were positioned at each end of the tube. The laser was placed next to the TRIGA reactor core and its 6150Å output monitored with a photomultiplier behind radiation shielding 10 meters away.

The mercury laser enhancement, an output signal increase due to the superposition of radiation on a laser, was achieved using pulses of peak flux 2.5×10^{15} n/cm^2-sec. The laser was pulsed electrically at 10 millisecond intervals through the high flux region of a reactor transient. The laser output increased to a peak just before the peak of the neutron flux, and then returned to an intensity below the starting intensity after the reactor

---

† This research supported by ERDA under contract AT(11-1) 2007

shutdown. A comparison of the maximum laser output to the starting laser output as shown in Figure 1 indicated as much as a 30-fold increase. Nuclear power input was accomplished via the $n(He^3,T)p$ reaction with He^3 instead of the more common He^4 as the major component of the laser gas mixture. The actual amount of power input attributed to the nuclear reaction was approximately one watt while the electrical input was approximately eight kilowatts for a two microsecond pulse. While the fractional power input due to the nuclear radiation is small, the enhancement is thought to result from pre-ionization of the gas which provides a significant improvement in breakdown characteristics and uniformity of the electrical discharge.

In summary this research has shown a nuclear enhancement for pulses of microsecond duration on a visible wavelength. Such enhancements may ultimately be important in high-power laser applications.

References:

1. See for instance, R. J. DeYoung, W. E. Wells, and G. H. Miley, Trans. of the Am. Nuclear Soc., 19, 1, P66 (1974). Also, T. Ganley, J. T. Verdeyen, and G. H. Miley, Appl. Phys. Lett., 18, 568 (1971).

2. J. A. Piper and C. E. Webb, Optics Comm., 13,2 (1975).

3. W. E. Wells, IEEE Conference Record 75CH0987-8-NPS, 2nd Conf. on Plasma Science (1975).

4. Laser Focus, 11, 6 (1975).

Figure 1. Nuclear Enhancement of Electrically Pulsed He-Hg Laser. Laser pulses, spaced 10 msec apart, are shown in the upper trace while the corresponding time history of the reactor flux appears in the lower trace.

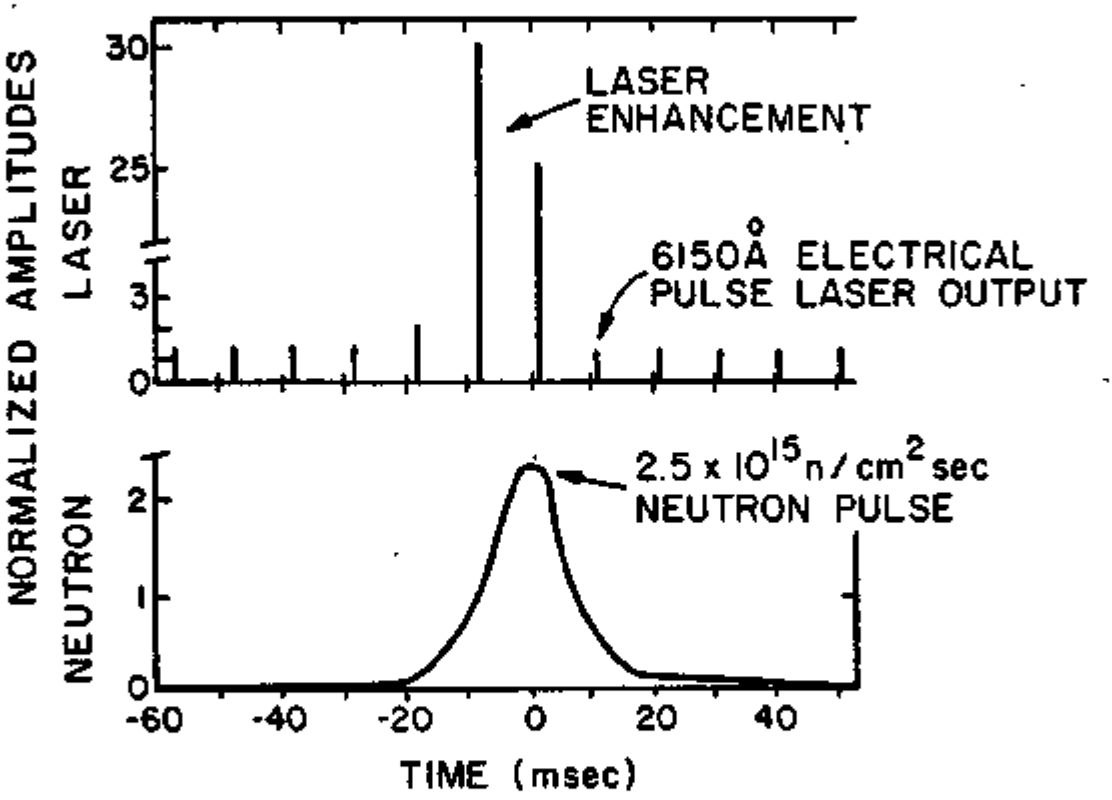

5 TORR He

0.02 TORR Hg

POSITIVE COLUMN LASER

Fig. 1. Nuclear Enhancement of Electrically Pulsed He-Hg Laser. Laser pulses, spaced 10 msec apart, are shown in the upper trace while the corresponding time history of the reactor flux appears in the lower trace.

APPENDIX B

POWER DEPOSITION ESTIMATES

Some calculations were made to acquire a feeling for the relative merits of some energy deposition methods useful to this type of research. A thorough examination of the ^{10}B reaction may be found in Ref. 1. The $^{3}He(n,p)T$ reaction is compared to the $^{10}B(n,\alpha)^{7}Li$ and $^{235}U(n,ff)$ reactions. To allow comparison, the reaction products in each case interact in a cylinder of 2.5 cm diameter and 30 cm length filled with helium. For the ^{10}B and ^{235}U reactions a thin layer is positioned on the inner surface of the cylinder. Then the reaction products lose energy moving through the foil to the surface before exciting the gas. The amount of energy deposited in the helium depends linearly on the helium pressure. For the ^{3}He reaction, reaction products are created in the gas and slow down as they lose energy. Therefore, the ^{3}He power deposition increases as the square of the helium pressure.

If the neutron absorption is small in the ^{10}B film, then the number of reactions taking place per second is:

$$R_{10_B} = n\sigma t A \phi = 5.6\times10^{16}/\text{sec} \qquad \text{(B-1)}$$

where

$n = 1.4\times10^{23}/cm^3$;

$\sigma = 4000$ b;

t = thickness of the film $= 1.74\times10^{-4}$cm;

A = the area of the film $= 236\ cm^2$;

ϕ = neutron flux $= 2.5\times10^{15}$ n/cm^2-sec.

In 92% of the reactions, the α particle starts with 1.5 MeV while the ^{7}Li has 0.85 MeV.[1] Assume that half the ions are created heading

in the right direction, and that they lose half their initial energy before reaching the gas. In addition, since the range of the ^{7}Li's in boron is 1.18×10^{-4}cm, less than the thickness of boron, assume that only those created in the inner half of the foil get into the gas.

The range in helium of the reaction products, then, is:[2]

$$\lambda_{\alpha} = \frac{1.6\times10^{3}}{p} \quad (cm)$$

$$\lambda_{Li} = \frac{3.9\times10^{2}}{p}$$

where p is the helium pressure in Torr. At a given pressure, the amount of energy deposited in the gas is

$$\Delta E_{\alpha} = 0.75\ \frac{r}{\lambda_{\alpha}} \tag{B-2}$$

$$\Delta E_{Li} = 0.43\ \frac{r}{\lambda_{Li}} \tag{B-3}$$

where r = average distance traveled through the gas by the ions.

Then the power deposited in the gas is:

$$Pwr = \frac{1}{2} R(\Delta E_{\alpha} + \frac{1}{2} \Delta E_{Li})\ 1.6\times10^{-13} \quad (In\ watts) \tag{B-4}$$

$$= \frac{1}{2} (5.6\times10^{16})(1.6\times10^{-13})(2.54)\left(\frac{P}{1.6\times10^{3}} + \frac{1}{2}\frac{P}{3.9\times10^{2}}\right)$$

$$= 21.7\ P \quad (P \leq 150\ Torr), \tag{B-5}$$

$$= 2250\left(\frac{P}{3.2\times10^{2}} + 1\right) \quad (150 < P \leq 630\ Torr), \tag{B-6}$$

$$= 6680\ watts \quad (630\ Torr < P \leq 1260\ Torr).$$

When the range of the α's is such that they can no longer reach the centerline, there is no point in going to higher pressures.

$^{235}U(n,ff)$ Reaction

The same approach was taken to arrive at the power deposition using a ^{235}U coating of 2×10^{-4}cm thickness. Two average fission fragments were considered rather than calculating ranges in helium for all of those possible.

$^{3}He(n,p)^{3}H$ Reaction

For this reaction, the approach is similar to the two previous cases.

The number of reactions per sec may be written:

$$R = n\sigma V\phi \qquad \text{(B-7)}$$

$$= 6.43 \times 10^{13}/\text{sec}$$

where $n = 3.5\times10^{16}P$ and P = pressure in Torr.

σ = 5000 barns

V = volume = 147 cm^3

$\phi = 2.5\times10^{15}$ n/cm^2-sec = thermal neutron flux.

Then for each proton and triton found, the energy deposited in the gas is:

$$\Delta E_{\alpha} = 6.5\times10^{-17}P \text{ (Joules)}. \qquad \text{(B-8)}$$

$$\Delta E_{T} = 2.15\times10^{-16}P \text{ (Joules)}. \qquad \text{(B-9)}$$

Then the power deposited is:

$$Pwr = 2.1\times10^{-5}P^2 \qquad (0 \leq P \leq 148 \text{ Torr}), \qquad \text{(B-10)}$$

$$= 4.2\times10^{-3}P^2\left(1 + \frac{500}{P}\right) \qquad (148 < P \leq 1480 \text{ Torr}), \qquad \text{(B-11)}$$

$$= 8.1\,P \qquad (1480 \text{ Torr} < P \leq 2300 \text{ Torr}). \qquad \text{(B-12)}$$

By 2300 Torr, the number of neutrons reaching the centerline is decreasing, making this an upper limit to the helium pressure.

The power deposited has been plotted in Fig. 1 to allow a comparison of the three approaches.

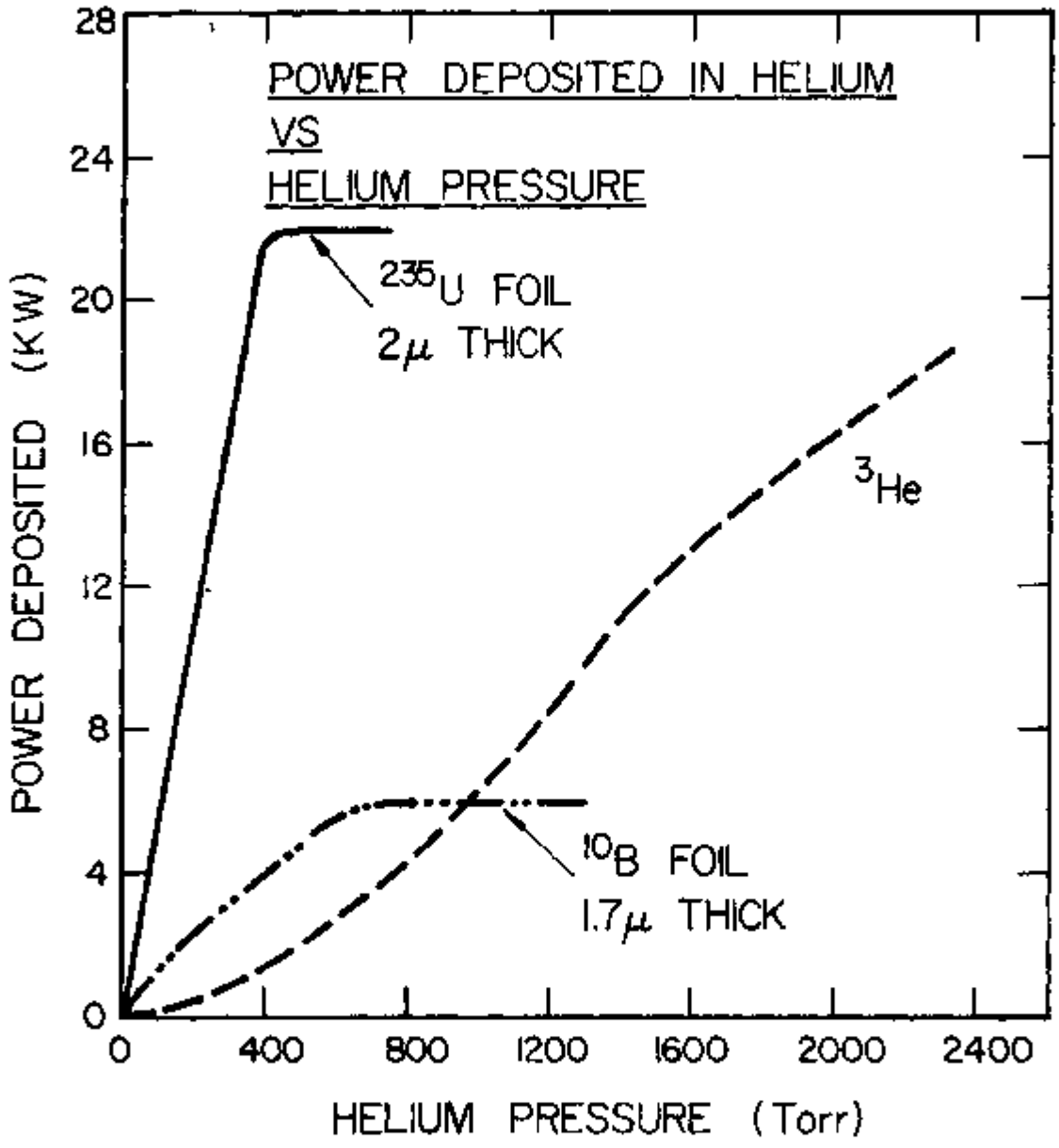

Fig. 1. Power deposited in helium by nuclear reaction products via ^{235}U, ^{10}B and ^{3}He.

LIST OF REFERENCES

1. J. C. Guyot, Ph.D. Thesis, University of Illinois (1972).

2. G. Friedlander, J. W. Kennedy and J. M. Miller, *Nuclear and Radiochemistry*, John Wiley and Sons, Inc., New York (1966).

APPENDIX C

A HELIUM MERCURY DIRECT NUCLEAR PUMPED LASER[†]

by

M. A. Akerman* and G. H. Miley
University of Illinois

and

D. A. McArthur
Sandia Laboratories

Abstract

A 6150-Å He-Hg laser, pumped solely by the $^{1}n(^{10}B,\alpha)^{7}Li$ nuclear reaction has been achieved using the Sandia SPRII reactor. The optimum conditions for lasing were 600 Torr total pressure with 2.5 mTorr Hg partial pressure, with a threshold for lasing of ~10^{16} n/cm^2-sec. This is the first visible wavelength laser having nuclear energy as its only source of excitation.

Introduction

Since the first direct nuclear pumped laser (DNPL) was discovered,[(1)] several others have been developed, all operating in the infrared.[(2)] We report the first demonstration of lasing on a visible wavelength where the pumping was accomplished solely with nuclear energy. A helium-mercury laser, pumped by the $^{1}n(^{10}B,\alpha)^{7}Li$ reaction,[(3)] and lasing at 6150 Å has been achieved. This is a transition in singly ionized mercury,[(4)] and the optimum conditions for lasing were found to be 600 Torr total pressure with ~2.5 mTorr mercury partial pressure.

Because the laser and detector were inaccessible in a radioactive area, and because of the relatively low power output and low pulse rate,

[†]This work was supported by the Division of Physical Research of U.S.E.R.D.A. and through the Sandia Laboratories by the Division of Military Applications of U.S.E.R.D.A.

an unequivocal test of lasing was necessary. A large decrease in signal strength when the back mirror of the laser was blocked provided this test. This result was in agreement with the indication of a threshold neutron flux of ~10^{16} n/cm^2-sec, based on an extrapolation of laser output versus neutron flux. Comparison tests employing an electrical laser showed that the output was strong enough that it would be visible to the human eye had the laser beam been directed outside the radiation control area.

In addition, lasing occurred for helium and mercury pressures predicted by gain measurements at the University of Illinois TRIGA reactor,[2] and with a threshold about twice the neutron flux available at Illinois.

This DNPL was discovered using the Sandia Pulsed Reactor (SPRII) to produce a high-flux pulse of neutrons.[5] Due to the inherent properties of such a machine, access to the experiment was limited and it was only possible to pulse the reactor about five times in one day. Hence, data were acquired more slowly than in typical electrically operated laser experiments. In one pulse of the SPRII reactor, however, up to 6×10^6 Joules are released. It is this enormous energy that sets the ultimate performance limits for DNPL's.

The peak nuclear laser output was approximately 1 mW. The estimate was made by comparing the peak nuclear laser output to the signal produced by a 4 mW He-Ne 6328-Å alignment laser. This measurement leads to an efficiency of ~10^{-6}%, based on a calculated 90 kW peak power deposited in the gas during a nuclear reactor pulse.

It should be stressed, however, that the present lasers were simply intended to prove lasing. Much improved performance should be possible with larger volume tubes designed to better utilize the nuclear radiation and concurrently it should be possible to come much nearer the 8%

quantum efficiency for the 6150-Å Hg transition. (Indeed there is a theoretical basis for expecting better overall efficiency with a DNPL than an equivalent electrical laser,[6] but this has yet to be demonstrated experimentally.

An earlier report of strong emission with a helium-mercury mixture by Andriakhin, et al.[7] of the Soviet Union initially led to the present work. However, we find no evidence for lasing at 6150 Å using their mercury pressure. In fact, we only find lasing at mercury pressures three orders of magnitude lower than those used in their experiment.

Experimental Setup

The laser used for this experiment was constructed of 2.7-cm I.D. Pyrex tube, 86-cm long. High temperature epoxy was used to seal thin Suprasil windows onto each end at Brewster's angle. A symmetrical hollow cathode and anode arrangement was employed to allow low-pressure electrical-operation for alignment.[8] The cathode was a 60-cm length of 2.54-cm O.D. titanium tubing coated on the inside with a 0.4-mg/cm^2 layer that was 66.8% ^{10}B by weight. This thickness corresponds to the range of an alpha particle in boron. The tube was wrapped with heater tapes to control the mercury partial pressure, and chromel-alumel thermocouples were used to measure the temperature of the tube. Two reservoirs contained a total of 79 mg of 67% isotopic abundant ^{202}Hg, enriched mercury being used to increase the gain over that which was possible with normal mercury.[9] The mercury partial pressure was determined from the temperature of the reservoir.[10]

The tube thus prepared was bolted into a rigid aluminum frame and mounted next to the SPRII as shown in Fig. 1. This reactor produces predominantly high-energy neutrons which must be moderated to interact

more efficiently with the boron coating. For this purpose a one-inch thick cylinder of polyethylene approximately 76-cm long was wrapped around the laser tube. A stopcock controlled from outside the reactor shielding provided isolation of the heated laser from the vacuum station. The vacuum pumping and ultra-high-purity helium fill were controlled by remotely operated solenoids and monitored using a thermocouple gauge and an MKS Baratron, respectively.

Mirrors were positioned to guide an alignment beam out of the reactor shielding through an 8-cm diameter opening, and then into a small room where a lens focused the light onto the photocathode of a GaAs photomultiplier shielded on all sides by four inches of lead brick. A three-meter radius of curvature mirror with a 99.9%-reflectivity dielectric-coating was used as the back mirror, while the flat output mirror had a reflectivity of 99%. A 30-Å bandwidth 6150-Å interference filter was inserted between the lens and the photomultiplier. A preamplifier was used between the photomultiplier and the oscilloscope to improve time response despite the necessary 20 meters of connecting coaxial cable.

Procedure

For approximately 40 minutes before nuclear reactor operation the laser was open to the vacuum pump. During this time laser temperature changes were made to assure stability at pulse time. Five minutes before nuclear reactor operation, helium was metered into the system and the stopcock at the laser was closed. This is the minimum time between filling and pulsing possible with the experimental apparatus employed, and the timing is considered important since longer delays may permit contamination of the laser gas. During nuclear reactor operation photomultiplier output was displayed on an oscilloscope and photographed. The

output of a high-energy neutron detector and a thermal neutron detector were also displayed and photographed. A signal initiated by reactor power level was used to trigger the oscilloscopes ~300 μs prior to the peak power point. Approximately one and a half hours elapsed between bursts to allow the reactor to cool. Thus, a graph such as the mercury pressure variation shown in the next section took more than a day to produce.

Results

Figure 2 allows comparison of the laser output to background noise. The typical output trace shown in Fig. 2 is composed of the laser light signal plus background noise. When the back mirror is blocked, the curve shown by the dotted line results. Other reactor pulses with the laser output mirror masked yield background radiation noise traces that vary from pulse to pulse. The observed upper and lower limits of the noise, are indicated by the brackets in Fig. 2. Several pulses were used to measure the noise, and the back mirror blocked signal. The noise composed of random spikes (not shown) superimposed on a more uniform envelope, peaks well before the maximum of the laser signal, indicating that it mainly arises from direct radiation associated with the fast neutron burst. In contrast, the laser output is more nearly in phase with the thermal neutron flux. This is expected since this component of the flux reacts with the ^{10}B liner. The light emitted with the back mirror blocked was too small to be observed above the random variation of the background radiation noise. The apparent offset between the thermal neutron flux and the laser output is thought to be due to a combination of the detector circuitry, and the fact that the thermal neutron detector was located slightly off the laser axis.

The mercury vapor pressure was varied in eight bursts between 2 and 10.2 mTorr. As shown in Fig. 3, the output increased with decreasing mercury partial pressure, at least to the lowest pressure achieved. The output should not increase much more at lower mercury pressure, since the reduction in available mercury atoms will eventually dominate. This behavior is not completely understood but is due to competing mechanisms for upper state population and is in basic agreement with gain measurements that show a peak between 3 and 4 mTorr.[2] The measurements were made at peak thermal neutron fluxes varying from 2.5×10^{16} n/cm^2-sec to 4.8×10^{16} n/cm^2-sec due to natural variation in nuclear reactor operation. Therefore, all points have been adjusted to an intermediate value of 3.8×10^{16} n/cm^2-sec.

A single nuclear reactor pulse at a total pressure of 300 Torr yielded laser output 40% lower than at 600 Torr. This is consistent with earlier gain measurements at Illinois,[2] which suggest that the 600-Torr region is near optimum. Time did not allow a complete pressure survey.

Figure 4 shows peak laser power output as a function of thermal neutron flux for similar mercury pressure. Due to the limited time only five data points are available. This does not allow more than a rough indication of the threshold. The two points at the optimum mercury pressure of 2.5 mTorr indicate a threshold of approximately 1.4×10^{16} n/cm^2-sec, while three points taken between 6 and 10 mTorr indicate a threshold of 2×10^{16} n/cm^2-sec.

In an attempt to achieve lasing with V. M. Andriakhin's stated conditions,[7] the laser was pumped down as usual, then filled with 350 Torr helium. The laser was heated to 162°C on the ends and 153°C in the active volume, while the mercury reservoirs were maintained at 150°C.

Heating brought the final pressure to approximately 505 Torr. The signal observed during a 6×10^{16} n/cm^2-sec pulse was essentially equivalent to normal background noise suggesting that no lasing took place. This result is again consistent with prior gain measurements at Illinois.[2]

Conclusions

No definitive study has been made of the pumping mechanism of the 6150-Å mercury ion laser at 600 Torr. The highest helium pressure for which electrical lasing has been reported is 40 Torr.[11] At this and lower pressures several studies have shown thermal-energy charge-transfer to be the dominant pumping mechanism.[11-17] The energy coincidence for the charge-exchange reaction can be seen in Fig. 5, as well as the mercury-ion levels important to the 6150-Å laser. At higher pressures, however, the formation of mercury and helium metastables, as well as He_2^+, provide additional channels for excitation and ionization. Such competing mechanisms are thought to be responsible for the decrease in laser output with increasing mercury partial pressure.[18]

While the efficiency reported is relatively low, considerable improvement should be possible using a laser tube designed specifically to optimize the charged-particle deposition in the gas as well as the output coupling. A direct measurement of the boron foil thickness, or the power deposited in the gas would allow a more accurate evaluation of the efficiency which is currently based on theoretical estimates.

The discovery of the 6150-Å helium-mercury DNPL demonstrates the feasibility of visible wavelengths DNPL's. An understanding of the mechanisms involved in pumping this laser may lead to higher efficiency visible and ultraviolet DNPL's which may ultimately be applied in the

areas of laser fusion, isotope separation, energy conversion and energy removal from gas core reactors.

Acknowledgment

We appreciate the glassblowing skill and precision that Keith A. Kuehl put into the basic construction of the pyrex tube and electrode assembly.

*Research submitted in partial fulfillment of Ph.D. requirements by one of the authors. (M.A.A.)

References

1. D. A. McArthur and P. B. Tollefsrud, *Appl. Phys. Letts.*, *26*, p. 181 (1974).

2. A table listing DNPL's discovered as of May, 1976, as well as He-Hg gain measurements may be found in: G. H. Miley, W. E. Wells, M. A. Akerman and J. Anderson, "Recent Nuclear Pumped Laser Results," The Third Conf. on Partially Ionized Plasmas, Princeton University (1976).

3. R. J. DeYoung, W. E. Wells, G. H. Miley and J. T. Verdeyen, *Appl. Phys. Letts.*, *28*, p. 519 (1976).

4. W. E. Bell, *Appl. Phys. Letts.*, *4*, p. 34 (1964).

5. L. L. Bonzon and J. A. Snyder, Sandia Pulsed Reactor II (SPRII) Experimenter's Manual, SLA-73-0551 (Nov. 1973).

6. R. H. Lo and G. H. Miley, "Electron Energy Distributions in a Helium Plasma Created by Nuclear Radiations," *IEEE Trans. on Plasma Science*, PS-2, p. 198 (1974).

7. V. H. Andriakhin, V. V. Vasil'nor, S. S. Krasilnikov, V. D. Pis'mennyi and V. E. Khvostinov, *JETP Letts.*, *12*, 2, p. 58 (1970).

8. H. Wieder, R. A. Myers, C. L. Fisher, C. G. Powell and J. Colombo, *Rev. Sci. Instr.*, *38*, 16, p. 1538 (1967).

9. R. L. Byer, W. E. Bell, E. Hodges and A. L. Bloom, *J. Opt. Soc. of Am.*, *55*, p. 1598 (1965).

10. *Handbook of Chemistry and Physics*, R. C. Weast, ed., Chemical Rubber Co., 18901 Cranwood Parkway, Cleveland, OH, 51st edition, p. D-145 (1970).

11. J. A. Piper and C. E. Webb, *Optics Communications*, *13*, p. 122 (1975).

12. D. J. Dyson, *Nature*, *207*, 4995, p. 361 (1965).

13. H. Kano, T. Shay and G. J. Collins, *Appl. Phys. Letts.*, *27*, p. 610 (1975).

14. I. P. Bogdanova, V. D. Marusin and V. E. Yakhontova, *Opt. Spectroscopy, 37*, p. 365 (1974).

15. A.Ferrario, *Opt. Communications, 7*, p. 376 (1973).

16. V. S. Aleinikov, *Opt. Spectroscopy, 28*, p. 15 (1970).

17. E. Graham, IV, M. A. Biondi and R. Johnsen, *Phys. Rev. A., 13*, p. 965 (1976).

18. M. A. Akerman, Ph.D. thesis, University of Illinois (1976).

Figure Captions

Figure 1. The 6150 Å DNPL is shown with the SPRII reactor, as well as the general experimental arrangement.

Figure 2. The laser output is compared to radiation noise and back mirror blocked signals. Random spikes appearing on oscilloscope traces have been smoothed out.

Figure 3. Laser output variation with mercury pressure.

Figure 4. Peak laser output vs. peak thermal neutron flux suggests a laser threshold corresponding to ~10^{16} thermal neutron/cm^2-sec.

Figure 5. The 6150-Å transition is shown along with several helium energy levels in a simplified energy level diagram.

Figures 1 through 4 are included in the main text of the thesis as Figs. 11, 23, 25 and 24, respectively.

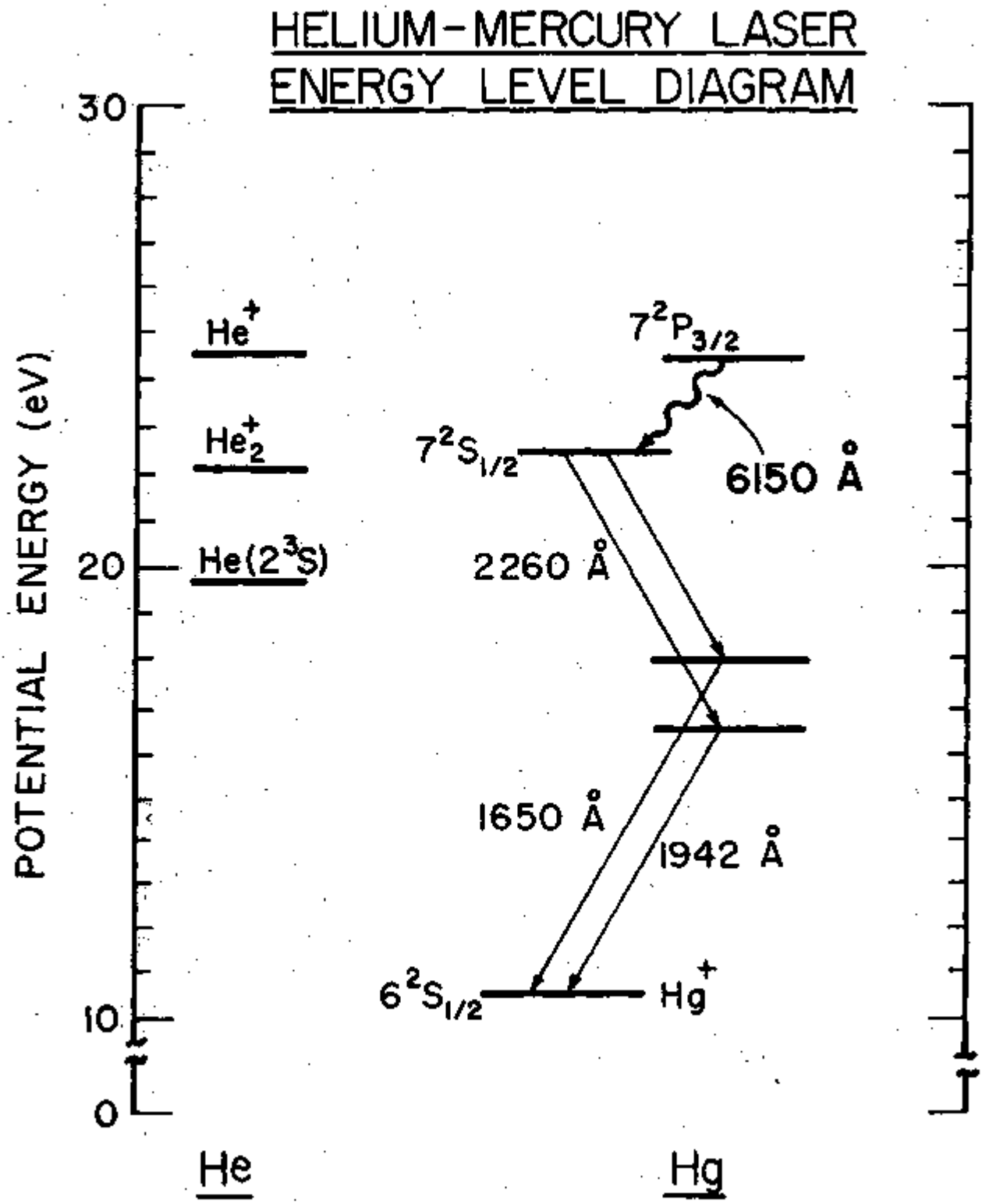

Fig. 5. The 6150-Å transition is shown along with several helium energy levels in a simplified energy level diagram.

VITA

M. Alfred Akerman was [redacted]

He earned the Bachelor of Science in Physics with Distinction from the University of Virginia in 1968.

After this he spent four years as a United States Naval Officer and Aviator during which time he flew multiengine, anti-submarine warfare aircraft. In 1972, he was promoted to the rank of lieutenant.

He earned the Master of Science degree from the University of Illinois in 1974 with a major in the Nuclear Engineering Program where he has been a research assistant since 1973.

He is married to Margo Lee [redacted] Akerman, formerly of Lincoln, Nebraska, and they have a daughter, Doriann.